

**Li AND B ANALYSIS BY NAA AND
He ISOTOPE MASS SPECTROMETRY**

**ULTRATRACE LITHIUM AND BORON ANALYSIS
BY NEUTRON ACTIVATION AND
HELIUM ISOTOPE MASS SPECTROMETRY**

**By
EDITH KAREN OLSON, BSc.**

*A Thesis
Submitted to the Faculty of Graduate Studies
in Partial Fulfilment of the Requirements
for the Degree
Master of Science*

**McMaster University
August 1990**

MASTER OF SCIENCE (1990)
(Physics)

McMASTER UNIVERSITY
Hamilton, Ontario

**TITLE: Ultratrace Lithium and Boron Analysis by Neutron Activation and Helium Isotope
Mass Spectrometry**

AUTHOR: Edith Karen Olson, B.A. (University of Calgary)

BSc. (Dalhousie University)

SUPERVISOR: Dr. W. B. Clarke

NUMBER OF PAGES: v, 65

ABSTRACT

The binding of the elements lithium and boron to human plasma proteins is investigated through the techniques of thermal neutron activation and helium isotope mass spectrometry. Since normal physiological levels of lithium and boron in blood and plasma are in the ultratrace (ppb) range, lithium in particular is frequently below the detection limit of many instruments. The success of the detection method used in this work is due to the extremely large cross section of ${}^6\text{Li}$ for the thermal neutron reaction ${}^6\text{Li}(n,{}^3\text{H}){}^4\text{He}$, and of ${}^{10}\text{B}$ for the thermal neutron reaction ${}^{10}\text{B}(n,\alpha){}^7\text{Li}$. The high sensitivity of the mass spectrometer, originally designed for oceanographic studies of helium isotopes and tritium, allows measurement of as little as 2×10^4 atoms of ${}^3\text{He}$ from the decay of tritium, and 2×10^{10} atoms of ${}^4\text{He}$ from alpha-particles.

It has frequently been stated that lithium does not bind to plasma proteins. However, our results clearly show that lithium does bind to a number of these proteins, at least *in vitro*. Boron is also shown to bind to proteins, with a pattern similar to that of lithium. Although a clear identification of the specific plasma proteins which bind lithium and boron must await further investigation, a number of possibilities are suggested here, based on the data obtained.

ACKNOWLEDGEMENTS

I would especially like to thank my supervisor, Dr. Brian Clarke, for his patience and guidance throughout the work on this thesis. I learned a great deal from him, and I am grateful for his encouragement. Special thanks are also due to Dr. Greg Downing of the National Institute of Standards and Technology for performing all the neutron irradiations, which were such an essential part of the whole process.

I would also like to thank Dr. Ronald Barr, for his enthusiasm and support, and most of all for his valuable contribution to the experiment. And finally, I would like to thank Roland Clarke and Bill Eismont for their help with the mass spectrometry; it was much appreciated.

Above all, this thesis is dedicated to my father, Dr. Nils Olson, and to the memory of my mother, Edith LaVerne Olson.

Table of Contents

Chapter 1 Introduction.....	1
1.1 Lithium.....	1
1.2 Boron.	7
Chapter 2 Lithium and Boron Analysis: Experimental Techniques.....	9
2.1 Introduction.....	9
2.2 Gel Filtration.....	10
2.3 Freeze-Drying and Evacuation.....	17
2.4 Neutron Activation.....	20
2.5 Mass Spectrometry.....	24
2.6 Gamma Counting.....	27
Chapter 3 Results and Discussion.....	29
3.1 Introduction.....	29
3.2 Interpretation of Mass Spectrometer Data.....	30
3.3 Thermal $^{39}\text{K}(n,\alpha)^{36}\text{Cl}$ Cross Section.....	33
3.4 Lithium and Boron in Whole Blood and Components.....	34
3.5 Protein Separations: Protein Profiles.....	37
3.6 Protein Separations: Lithium and Boron Profiles.....	41
3.7 Discussion.....	53
Chapter 4 Summary.....	59
Bibliography.....	61

Chapter 1

Introduction

An understanding of how metal ions interact with various biological systems is of great importance in medicine, biology and chemistry, since in many cases, these interactions serve to regulate vital functions such as enzyme action, which are necessary to life. For example, many metal ions are known to bind to proteins. A number of these elements are known to be, or are now thought to be, essential in human and animal nutrition. These include certain metals, such as nickel, chromium, selenium and arsenic, which are normally regarded as toxins, but which appear to be essential in trace (ppm) or ultratrace (ppb) quantities. In this thesis, the binding of lithium and boron to human plasma proteins is investigated. These two elements are not presently regarded as essential, although lithium has significant therapeutic value in the treatment of manic depression and some hematological disorders. The analysis makes use of thermal neutron activation, through the reactions ${}^6\text{Li}(n,{}^3\text{H}){}^4\text{He}$ and ${}^{10}\text{B}(n,\alpha){}^7\text{Li}$, and subsequent helium isotope mass spectrometry to measure ultratrace amounts of lithium and boron in plasma protein fractions.

1.1 Lithium

The use of lithium in treating manic-depressive psychosis and certain other psychiatric disorders is well documented, and has been the subject of considerable research ever since Cade's ^{1,2} discovery of the treatment in 1949. Since then, much of the research has been focused on the mechanism through which lithium

accomplishes this, that is, the pharmacological effects of lithium on biological systems. A discussion of the biological and pharmacological properties of lithium is beyond the scope of this thesis; therefore, the reader is referred to a number of reviews and books³⁻⁷. There is also an extensive literature in medical, biological and pharmacological journals.^{8,9} However, there has been relatively little research on normal physiological levels of lithium, its essentiality as a trace element, or on protein binding. Although the present work is concerned with this last aspect, the other two are briefly discussed since they are closely related.

In order to be effective in treating mania or manic depression, lithium must be given in relatively large doses. When lithium, usually in the form of lithium carbonate, is ingested, it enters the bloodstream within a few hours, where an equilibrium distribution between red cells and plasma is quickly established. Various other organs also accumulate lithium at varying rates. Lithium is also rapidly excreted, almost exclusively through the kidneys. The usual doses of 1200 - 1800 mg of lithium carbonate per day lead to plasma lithium levels of 0.9 - 1.4 mEq/L (1 mEq/L = 6.9 µg/ml), about three orders of magnitude higher than normal levels. The borderline of toxicity for lithium is generally considered to be ~1.5 - 2.0 mEq/L¹⁰, so that careful monitoring of the patient's plasma lithium is an essential part of treatment. It follows that a great deal of interest in lithium has been centred on its metabolic effects at therapeutic levels. At these concentrations, plasma lithium is easily monitored by such conventional techniques as atomic absorption or emission spectrometry.

Part of the reason for the lack of work on physiological lithium levels in human blood and plasma may be due to the fact that under normal (non-therapeutic) conditions, lithium is found in ultratrace amounts, and is therefore frequently below the detection limit of many instruments without extensive chemical processing. At

these levels, any contamination due to handling or processing may be enough to lead to variable results. A survey of the available literature is indicative of this variability. For example, Hamilton et al.¹¹ analyzed four samples of a composite of 2500 individual whole blood samples from donors in the U.K. by spark source mass spectrometry, and obtained a mean value of 2.0 ± 0.4 ng/g wet weight. They also quote a mean value of 6.0 ± 2.0 ng/g wet weight from 101 individual samples, again from the U.K. More recently, Clarke et al. reported a range of 1.54 - 4.42 ng/g dry weight ($\sim 0.32 - 0.90$ ng/g wet weight), with an average of 2.64 ± 0.94 ng/g dry weight ($\sim 0.54 \pm 0.19$ ng/g wet weight)¹² in seven samples of whole blood, and a range of 0.30 - 0.96 ng/g wet weight in fourteen samples of whole blood, with an average of 0.58 ± 0.06 ng/g wet weight¹³. Analysis was by neutron activation and helium isotope mass spectrometry, which will be discussed in more detail later.

Other studies include one by Bourret et al.¹⁴, which quoted a range in blood serum (plasma in which the fibrinogen is removed by clotting) of 2 - 17 ng/ml (2.1 - 17.5 ng/g wet weight) and a mean of 8 ng/ml (8.2 ng/g). Luan et al.¹⁵ analyzed seven serum and fourteen whole blood samples from donors in China by graphite furnace atomic absorption spectrometry. They reported a range of 1.2 - 7.3 ng/ml (1.24 - 7.52 ng/g wet weight), with a mean of 2.8 ± 2.1 (S.D.) ng/ml (2.88 ± 2.16 ng/g) for serum, and a range of 0.6 - 6.1 ng/ml (0.64 - 6.47 ng/g wet weight), with a mean of 2.1 ± 1.4 ng/ml (2.23 ± 1.48 ng/g) for whole blood. The detection limit for this method was given as 0.24 ng/ml in undiluted samples. It can be seen that the values quoted by Clarke et al. are considerably lower than those of Hamilton et al. or Luan et al., except for the lower end of the range reported by the latter for whole blood. Whether these differences are due to instrument effects,

dietary intake, geographical location, contamination, or a combination of all of the above, is unclear.

That lithium levels in drinking water can influence body lithium levels is illustrated in a brief report by Zaldivar¹⁶ of a region in northern Chile, where lithium in certain streams may be as high as 5170 ng/g (the average for North American streams is ~ 1.1 ng/g ¹⁷). A study of subjects from this region showed plasma lithium levels as high as 90 ng/g (no data given for whole blood), still well below the therapeutic level, but substantially higher than any of the values quoted previously.

Another related topic which has been relatively neglected is whether or not lithium is an essential trace element in humans or any other animal species. Mertz¹⁸ gives a definition of essentiality as follows:

" An element is essential when a deficient intake consistently results in an impairment of a function from optimal to suboptimal and when supplementation with physiological levels of this element, but not of others, prevents or cures this impairment."

Mertz goes on to state that an element is generally acknowledged to be essential when demonstrated by more than one independent investigator, and in more than one animal species. Normally, there is a fairly narrow optimal range which varies from element to element. It should be noted that manic depressive psychosis is not the result of a lithium deficiency, a fact evidenced by the extremely high concentrations required to treat the condition, as opposed to normal physiological concentrations.

It has been known for some time that such trace and ultratrace elements as iron, copper, zinc, manganese and cobalt are essential to many biological functions and processes. More recently, it has been acknowledged that several additional ultratrace elements such as silicon, chromium, vanadium, nickel, selenium and

arsenic, are also essential elements in at least some animal species¹⁸⁻²⁰. Previously, most of these were considered only as environmental toxins. Some evidence for the essentiality of lithium may be found in the work of Patt et al.²¹, Burt²² and Pickett²³ on the effects of low-lithium diets in rats. They noted some reproductive impairment, and also that concentrations of lithium in the pituitary and adrenal glands remained constant, regardless of the lithium concentration in the diet. Further evidence is reported in the work of Barr et al.²⁴, in which it was observed that growth rates of human bone marrow cells *in vitro* were stimulated by ultratrace amounts of lithium. This suggests that lithium has a role in human blood cell formation. A review of related works is given in Barr and Galbraith²⁵. Clarke et al.^{12, 17} have also pointed out that concentrations of lithium in blood fall into a fairly narrow range, which again is suggestive of essentiality.

Part of the difficulty in determining essentiality of lithium is due to the fact that although lithium is not a common element anywhere, it is nevertheless widely distributed. This wide distribution, coupled with the minute quantities apparently required, if it is indeed essential, make it very difficult to induce a true deficiency, even under strictly controlled laboratory conditions.^{22,23}

If lithium is an essential ultratrace element, then the question arises as to the biological mechanisms involved. One of these mechanisms by which essential elements are transported is the binding of metal ions to plasma and other proteins, as noted earlier. Herein is the main focus of the present work; to attempt to determine if lithium, along with boron, is bound to any plasma protein(s).

It is well known that iron is bound to the plasma proteins transferrin and ferritin^{26,27}, copper to ceruloplasmin, and zinc to α_2 -macroglobulin and albumin^{27,28}. There has also been research on the binding of the non-essential

element aluminum to transferrin²⁹⁻³², after it was discovered that aluminum toxicity was responsible for a form of dementia suffered by some patients undergoing dialysis for kidney failure. Recently, it has been determined that selenium is bound to α_2 - and β_1 - globulins and lipoproteins^{33,34}, and nickel to albumin and a macroglobulin called nickeloplasmin^{27,35}. Vanadium apparently binds to transferrin^{19,36}. There are others, but these examples serve to point to the considerable interest in the binding of metal ions to human plasma proteins. In contrast, there appears to have been virtually no interest in the possibility of lithium binding to any of these proteins, or to other smaller protein constituents such as peptides. The only reports discovered so far, which deal specifically with the binding of the alkali metals (Na, K, Li) to proteins, date from the 1950's^{37,38}. In their experiments, the authors used potential measurements across electronegative collodion membranes as an indication of protein binding. A decrease in ion activity in a protein solution with respect to reference solutions of NaCl, KCl (and also LiCl in the second work) was taken as evidence of binding. Carr³⁷ determined that Na⁺ and K⁺ appeared to bind to fibrinogen (Cohn Fraction I, named after the researcher who pioneered a method of separating proteins with ethanol³⁹), to Cohn Fraction III proteins (ex: β_1 -lipoproteins, plasminogen, and α - and β - globulins), and to part of Cohn Fraction IV (ex: α_1 -lipoprotein and phosphatase), but not to albumin. Carr and Engelstad³⁸ claimed that Na⁺, K⁺ and Li⁺ were bound to phosvitin (a chicken plasma protein with a high phosphorus content), casein (a milk protein), and a phosphorus-containing peptide obtained from casein. They determined that the extent of binding was Li>Na>K, and that binding was pH-dependent, with no binding observed below pH 5.7. It is difficult to know how to interpret these findings, especially those for lithium, since the lithium concentration used was 11.8

mmol/l, which is about ten times therapeutic levels. It may be that proteins would behave differently when exposed to higher or lower than normal plasma concentrations. It should also be noted that the proteins were primarily obtained by Cohn's method³⁹, which can cause denaturation⁴⁰. How this would affect metal binding is uncertain.

Aside from these observations, other researchers^{41,42} decades ago stated that lithium was not bound to plasma proteins. This continues to be the position taken today^{10,43,44}.

1.2 Boron

If the study of physiological levels of lithium has been relatively neglected, studies of physiological levels of boron in humans and other species are almost non-existent. Since boron can also be detected by thermal neutron activation and helium isotope mass spectrometry, the present work is also concerned with the distribution of boron in human plasma proteins.

Undoubtedly, part of the reason for this neglect is that while boron has long been known to be essential to plant growth, there is no evidence so far to indicate that it is essential to any animal species^{20,27}. It appears that the only available study which attempted to determine the essentiality of boron is one by Hove et al.⁴⁵ in 1939. Young rats were fed a low-boron diet which supplied 0.155 ppm of boron for an average intake of 0.8 $\mu\text{g/day/rat}$, and their growth rates were compared with animals fed the same diet supplemented with 100 μg of boron/75 ml of water. The authors observed no differences in growth rates with diet and concluded that if boron were essential, then a diet supplying 0.8 $\mu\text{g/day}$ was sufficient. As with lithium, boron is relatively rare but ubiquitous, so it would also

be difficult to induce boron deficiency, especially if boron were required in ultratrace quantities.

A few studies of boron levels in human blood have been done, but like the lithium studies, the results are variable. The earliest systematic study was by Imbus et al.⁴⁶ in 1963. They report a mean value of 114 ng/g wet weight, with a range of 39 - 365 ng/g wet weight for 147 subjects from several U.S. cities. Hamilton et al.¹¹ reported a mean value of 400 ng/g wet weight, although this was considered a preliminary value due to interference in the mass spectral lines. Lastly, Clarke et al.^{12,13} reported a mean of 97 ± 22 ng/g dry weight (20 ± 5 ng/g wet weight), with a range of 79 - 138 ng/g dry weight (16 - 28 ng/g wet weight) in seven whole blood samples, and a mean of 31 ng/g wet weight, with a range of 15 - 80 ng/g wet weight in fourteen whole blood samples. Again, these values are lower than those of the first two authors quoted. As far as can be determined, no work has been done on protein binding of boron.

The major interest in boron at present is in the use of the isotope ^{10}B in cancer therapy, through the thermal neutron reaction $^{10}\text{B}(n,\alpha)^7\text{Li}$ ⁴⁷. It is possible that more work on the interaction of boron with various biological systems will be undertaken as a result.

Chapter 2 of this thesis describes the experimental techniques used in the analysis. Several steps are involved, including gel filtration to separate the proteins, freeze-drying, neutron activation, helium isotope mass spectrometry, and gamma-counting.

Chapter 3 discusses the results of two separate experiments, while Chapter 4 is a brief summary of these results, and the conclusions drawn from them.

Chapter 2

Lithium and Boron Analysis Experimental Methods

2.1 Introduction

Given that lithium and boron are present in plasma in ultratrace quantities, two major considerations in the experiment were avoiding contamination due to handling and environmental tritium to the greatest extent possible, and minimizing chemical processing of the samples.

In the method described below, the second criterion is certainly met, since the only chemical treatment is removal of the water in the samples by freeze-drying. The problem of initial sample contamination by environmental tritium, which adds to the apparent lithium in the samples, and by lithium and boron from dust particles, is more difficult to control, but can be corrected for. Environmental tritium can be measured through the use of non-irradiated samples representative of the material to be irradiated. Direct contamination by lithium and boron can be corrected for through the use of irradiated blanks. Blanks are simply empty liners (small polyethylene tubes sealed at one end) which are taken through the same steps as the other samples. In addition, all materials coming in contact with the blood and plasma samples were made of various kinds of plastic, except for the syringe needle used when drawing the blood, and a stainless steel spatula for scooping the freeze-dried material into liners. Plastic materials were cleaned by first soaking briefly in dilute HNO_3 to remove surface contamination. They were then rinsed thoroughly

with distilled water, followed by acetone or methanol, and dried with nitrogen gas in a cleaned plastic container.

Two separate experiments were conducted, each consisting of five stages: (1) separation of the plasma proteins by molecular weight by gel filtration; (2) freeze-drying, placement of the freeze-dried samples in lead tubes, and evacuation under high vacuum; (3) neutron activation in a highly thermalized neutron flux; (4) helium isotope mass spectrometry; (5) gamma-counting of the lead tubes to determine variations in the neutron flux reaching the samples.

2.2 Gel Filtration

Gel filtration, also known as gel chromatography, or molecular sieve chromatography, is a process in which large molecules such as proteins are separated according to size by passing them through a column packed with a porous gel. Depending on their size, the molecules spend varying amounts of time in the pores of the gel (stationary phase) before passing out of the column. The largest molecules are completely excluded from the gel pores, and are confined to the so-called mobile phase outside the gel volume, with the upper limit for exclusion depending on the type of gel used. These large molecules will therefore be eluted first, in what is called the void volume. The smallest molecules, and ions, spend the most time in the stationary phase and so are eluted last. An ionic solution such as NaCl, KCl, or a buffer solution is normally used as the solvent, hereafter referred to as the eluant. The purpose of these solutions is to prevent the proteins from binding to the gel particles, and thus being trapped in the column. This can occur because the gel has a number of charged groups in its structure, which will attract oppositely charged protein molecules, unless an ionic solution is added to counteract this tendency. A detailed study of the elution behaviour of proteins in

the gel Sephadex G-200 (Pharmacia, Sweden), the same gel used in our experiments, was undertaken by Andrews⁴⁸ in 1965. The study showed a good correlation between elution volume and molecular weight for a wide range of proteins.

Sephadex G-200 is a type of gel which has been widely used to perform separations of a group of large molecules such as plasma proteins. This gel is loosely cross-linked, with an exclusion limit of about 600,000 daltons (1 dalton = 1 amu). The lower limit is about 5000 daltons.⁴⁹ This range allows proteins of various sizes to be eluted in distinct groups, rather than all at once as they would be with a tightly cross-linked gel. The degree of cross-linking of the polymer chains which make up the gel determines the exclusion limit, so that gels with a low degree of cross-linking have the highest exclusion limits.

Typically, most of the proteins passed through Sephadex G-200 are eluted in three peaks, followed by a fourth peak, called the "ion peak", which contains various ions, small proteins, peptides and sugars, all with molecular weights less than the lower limit quoted above. The technique of gel filtration has been extensively used by researchers to study metal ion binding to plasma and other proteins.^{28,30-32,34,50-54} Its main advantage is that it requires no chemical processing of the samples.

Commercially available gel filtration columns were considered unsuitable, since they are normally made of borosilicate glass. Therefore, a length of clear polycarbonate tubing (i.d. = 1.905 cm, length = 173 cm) was substituted. Since resolution of two separated zones increases as the square root of the column length, a long column is necessary for good resolution. Also, since a sample volume of 1%-5% of gel bed volume is recommended for optimum resolution, a long column was required to accommodate the large (18-20 g) samples which were applied.

Initially, as in the case of all other plastic material, the tube was soaked in dilute HNO_3 and distilled water, then rinsed with methanol, as described previously. For subsequent uses, the column was rinsed quickly with HNO_3 , and then filled with distilled water until ready to use. In between experiments, it was cleaned, dried and wrapped in plastic.

The top and bottom pieces were made from the tops of 100 ml wide mouth polyethylene squeeze bottles. At the bottom of the column, inside the cap, was a perforated polyethylene disc, with a disc of fine nylon mesh underneath to hold the gel in place. Tygon tubing of various sizes was used for the eluant inlet and outlet, and the air vent at the top. An inverted 500 ml polyethylene squeeze bottle fitted with a funnel held the eluant supply, which was fed into the column by gravity feed. Plastic clamps at various locations allowed the flow to be shut off, or the column opened and closed whenever necessary (see Figure 2.1). Although of relatively simple construction, the column performed consistently well during both gel filtration experiments.

About 25 g of the gel, which is supplied in dry bead form (average diameter 40 - 120 μ) was soaked in distilled water in a clean, covered plastic beaker for a minimum of three days, during which time the gel swelled considerably, filling a volume of $\sim 30 - 40$ ml/g of dry gel⁴⁹. The gel mixture was stirred occasionally, and part of the water replaced each day with fresh distilled water. Just prior to packing the column, part of the water was replaced with eluant, and the gel mixture was degassed under low pressure. The purpose of degassing was to remove air bubbles which could interfere with the proper packing and subsequent operation of the gel column. After degassing, the gel mixture was carefully poured down a plastic stirring rod into the column and allowed to settle. More gel was added at this stage as required. When the gel bed was stabilized, the flow of eluant

was started, and several column volumes were passed through the gel bed to equilibrate it. A column volume was taken to be about 380 ml, which was the approximate volume required to elute the protein peaks. In the first experiment, four column volumes of eluant were passed through before placing the plasma on the column. In the second experiment, eight column volumes were passed through before adding the plasma.

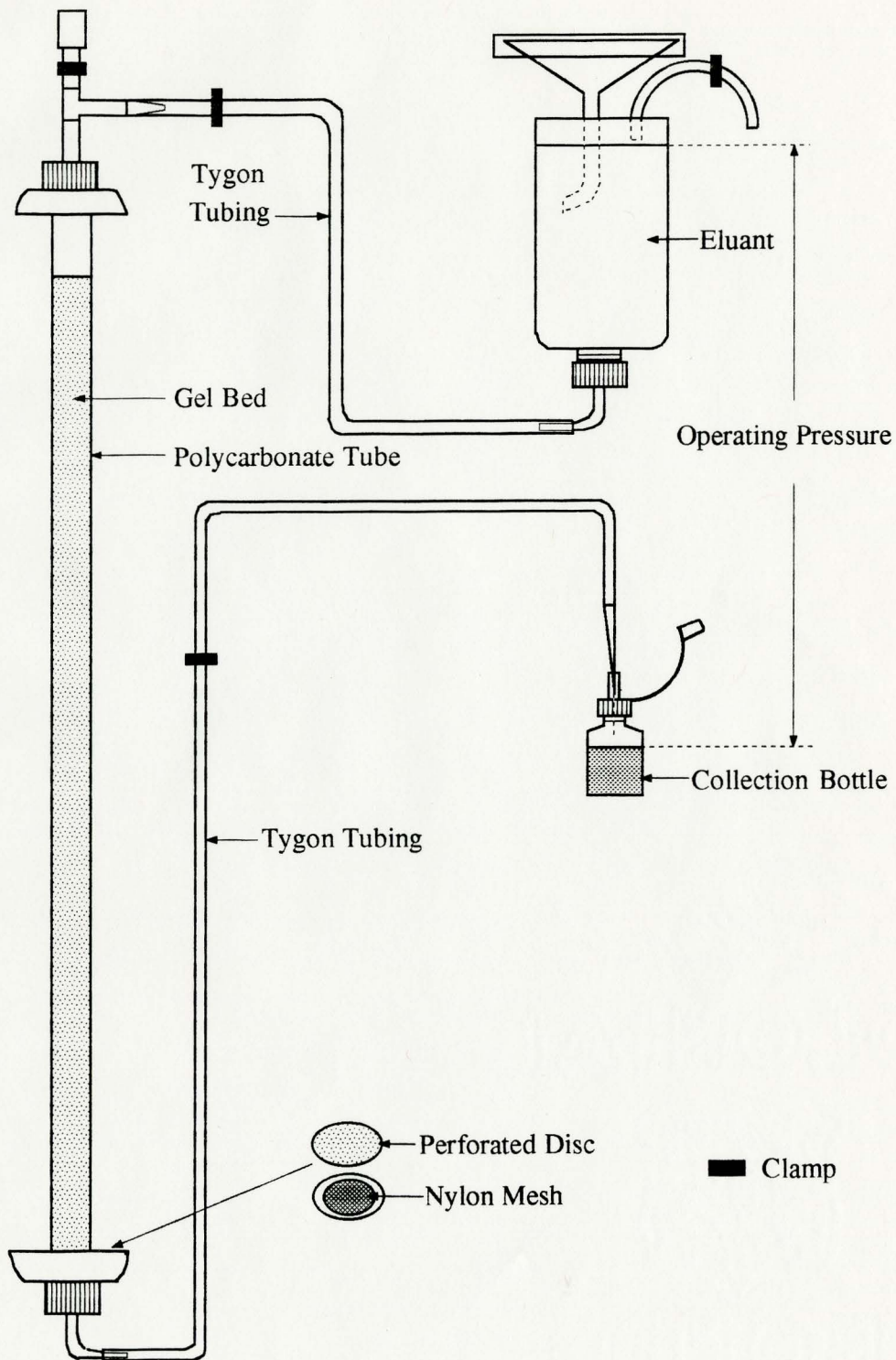
During the equilibration process, the column was moved to a cold room (4 °C) at the McMaster Medical Centre. Running the column in the cold room prevented temperature changes which can cause the formation of air bubbles in the gel bed, and also slowed bacterial growth. This was an important consideration, since no antibacterial agents were added to the eluant because of the possibility of contamination. Once in the cold room, the column was kept running until ready for use.

Two separations of plasma proteins were performed in the course of the experiment. For the first, the eluant used was phosphate-buffered saline (PBS) with pH ~ 7.4 and concentration 0.15 M. It consisted of 8.03 g NaCl, 0.20 g KCl, 1.14 g Na₂HPO₄ and 0.199 g KH₂PO₄ in 1000 g of solution. All chemicals were Gold Label grade (99.99%+, Aldrich Chemical Co. Milwaukee, Wis.). For the second separation, the eluant consisted of 0.08 M KCl, or 5.964 g analytical grade KCl/l, with pH ~ 7.0. Deionized distilled water was used to prepare all solutions.

Initial column flow rates at room temperature (23 °C) were about 17 ml/hr in the first case, and about 13 ml/hr in the second case. This latter rate decreased to 10 ml/hr after 24 hours of running. The different rates were most likely due to differences in column packing. Once in the cold room, rates decreased to 10 ml/hr with the PBS eluant, and 4 ml/hr with the KCl eluant. Differing viscosities of the

Figure 2.1. Gel filtration column.

14a



the two solutions at low temperature may have been responsible for the larger decrease in flow observed with the KCl solution.

Collection bottles for the protein fractions were 15 or 30 ml polyethylene snap top drop dispenser bottles. Prior to use, the bottles were cleaned as described previously, weighed, numbered, and placed in closed plastic containers. Liners (length 6.0 cm, o.d. 0.60 cm, thickness 0.03 cm, average weight 240 mg) were prepared from Alathon 1645 polyethylene tubing (Dupont Co., Wilmington, Del.), which is known to be low in lithium and boron. It also rapidly releases ^3He from the decay of tritium, and ^4He from α -particles to the gas phase inside the irradiation container¹³. In preparation for the experiment, the liners were "fringed" by making about fifteen cuts around the top, then cleaned, weighed and placed in numbered polypropylene tubes inside a plastic container and bag. The purpose of the fringes was to allow the top to be folded down with tweezers to hold the contents in place.

For each separation, 55 ml of blood were drawn from the same donor, and transferred to a centrifuge tube containing 0.1 ml (2500 units) of the anticoagulant calcium heparin. Three samples of whole blood of about 0.8 - 1.0 g each were pipetted into liners and weighed. The remainder of the blood was centrifuged to separate plasma from red cells. Afterwards, three samples of plasma, about 0.8 - 1.0 g each were also pipetted into liners and weighed. Most of the remaining plasma was pipetted into a preweighed 30 ml Teflon bottle. A fourth plasma sample was made of the residue, except for about 0.3 ml on top of the red cell layer. Lastly, three red cell samples, of about 1.0 g each were pipetted into liners and weighed. The rest was discarded. The plasma plus Teflon bottle plus Teflon tubing fitted over the bottle's spout was weighed, and then taken to the cold room

and left for two hours to allow it to reach room temperature. The blood and plasma samples in the liners were stored at -20°C until they could be freeze-dried.

In preparation for adding the plasma, the eluant flow to the column was stopped, and the eluant on top of the gel bed was removed, either by allowing it to drain out (first experiment), or by removing it with a pipette (second experiment). In both cases, care was taken not to let the gel bed run dry. The column outlet was shut off, and the plasma was carefully added to the top of the gel bed directly from the Teflon container.

After adding the plasma, the column outlet was opened, and the eluant allowed to flow until the plasma had completely sunk into the gel bed. The flow was stopped again, and eluant was slowly added to the top of the column to the point of overflowing, and the column was capped. Before restarting the flow, air which had collected under the cap was removed by tapping the column. Sample collecting began immediately ^{as} the flow was restarted. The Teflon bottle with any remaining plasma was returned to the laboratory and weighed.

For the first protein separation, twenty-eight fractions of about 20 g each were collected in the 30 ml bottles, while for the second separation, fifty-six samples of about 12 g each were collected in the 15 ml bottles. Flow was maintained by gravity feed as noted earlier. The maximum recommended operating pressure for the gel type, equivalent to 16 cm between free surfaces (see Figure 2.1) was maintained by periodically topping up the eluant bottle. Samples were collected manually instead of with a fraction collector to avoid exposing the samples to the open air in test tubes, and hence to evaporation and possible contamination. With this arrangement, evaporation was found to be negligible. Collection intervals ranged from two to three hours depending on the column flow rate.

As each sample bottle was filled, it was immediately capped and placed in a closed plastic container, inside a plastic bag. Since the collection took from seven to ten days, allowing for shutdown at night, the accumulated samples were periodically taken to the lab, allowed to come to room temperature (~ 2 hr) to remove any surface condensation, and then weighed. Samples from the first separation were placed in a freezer after weighing, while those from the second were returned to the cold room until collecting was finished. Only after all fifty-six samples were collected and weighed were they placed in the freezer.

2.3 Freeze-Drying and Evacuation

While the protein fractions were being collected, the frozen blood and plasma samples were freeze-dried along with standards, which were prepared from aqueous solutions containing known amounts of lithium and boron. Later, the frozen samples from the first protein separation were arranged on a rack with the tops on but the snap top open, placed in a stainless steel container, lowered into an insulated bucket containing liquid N_2 , and left for an hour before placing in the freeze-dryer, which had been previously cooled to $-20^{\circ}C$.

Despite the initial liquid N_2 treatment, part of the contents of a few of the bottles on the upper rack, especially those containing significant amounts of protein, escaped as the temperature reached $0^{\circ}C$. None of the bottles on the lower rack "spouted" to any extent, presumably because the temperature was slightly lower. The loss was determined after freeze-drying was complete by weighing the bottles with and without the escaped material, which was deposited on the cap of the bottle it came from. The liquid N_2 pre-treatment was not used in subsequent freeze-drying operations, since it seemed to be of no benefit.

The samples from the second separation were taken directly from the freezer, placed on the rack with their tops off this time, and lowered into the pre-cooled freeze-dryer chamber. As the samples containing only KCl solution evaporated, a light, fluffy white powder remained, small amounts of which escaped from some of the bottles. Fortunately, the loss amounted to only a few milligrams.

When freeze-drying was complete, those samples already in liners, i.e. the standards and blood and plasma samples, were weighed and placed in numbered lead tubes (99.99% pure, length 10.5 cm, o.d 0.975 cm, thickness 0.20 cm), which were pinch-sealed at one end. The tubes were clamped to a high vacuum line, and pumped out for at least 24 hours to a pressure of 10^{-5} Torr or less to remove dissolved atmospheric He. After pumping out, the tubes were again pinch-sealed just above the liner top, forming a leakproof container for irradiation. After this stage, contamination of lithium and boron on the outside of the lead containers is not a concern, since the ranges in lead of tritons from the ${}^6\text{Li}(n,{}^3\text{H}){}^4\text{He}$ reaction, and α -particles from the ${}^{10}\text{B}(n,\alpha){}^7\text{Li}$ reaction, are very small compared to the thickness of the lead tubes.

The lead containers also have excellent integrity against leakage. Tests¹³ have shown that even after a year, samples sealed in non-irradiated tubes showed no detectable ${}^4\text{He}$ above the mass spectrometer inlet line blank. The small amount of ${}^3\text{He}$ present in excess of the mass spectrometer inlet line blank can be attributed to existing tritium in the sample and liner. Hence, when properly sealed, the tubes are impervious to atmospheric He or outward loss of He from the irradiated samples.

Upon completion of freeze-drying of the protein fractions, the bottles were removed from the freeze dryer, recapped, and stored in a closed container for about

two hours to allow the bottles to rehydrate before weighing. It had been noted previously that the polyethylene bottles would gain or lose an average of 0.5 mg in mass, depending on the humidity.

Initially, an attempt was made to reconstitute the dry protein fractions by dissolving them in 2 ml of distilled water, producing a concentrated solution which could be pipetted into liners and freeze-dried again before pumping out. However, this proved to be unworkable, since some of the protein samples would not dissolve in water. Therefore out of twenty-eight fractions from the first separation, only the first twelve were reconstituted, and the proteins mixed as well as possible. The remaining sixteen fractions were ground gently with a stainless steel spatula, and the resulting dry powder was scooped into the liners. The contents of each bottle were divided between two liners, one to be irradiated, and the other to be kept back to monitor tritium levels.

The fifty-six protein fractions from the second separation were also ground with a spatula and scooped into liners. This time, only a few selected samples were kept back for measurement of initial tritium. These included a sample of KCl eluant, and part of a sample from each of the three protein peaks. One sample of calcium heparin, two each of whole blood and plasma, and two standards and blanks were also kept back. In the process of scooping out the powder, a small portion of it was invariably lost. This was more noticeable in the second set of fractions, many of which consisted of a light, fluffy powder which clung to the walls of the bottle and to the spatula. However, as the bottles were weighed initially, and again after the dry samples were removed, the losses could be accounted for. It was at this stage that the protein samples were most vulnerable to contamination, both from environmental tritium and from dust. As each liner plus

contents was weighed, it was placed in a numbered lead tube, attached to the high vacuum line, and pumped out as described previously.

2.4 Neutron Activation

The success of helium isotope mass spectrometry in measuring lithium and boron in various materials is made possible by the reactions ${}^6\text{Li}(n,{}^3\text{H}){}^4\text{He}$, and ${}^{10}\text{B}(n,\alpha){}^7\text{Li}$, both of which have very large cross sections ($\sigma_{\text{th}} = 940$ barn and $\sigma_{\text{th}} = 3837$ barn respectively) for thermal neutrons (.025 eV). The ${}^4\text{He}$ comes from the α -particles, with a small additional amount from the lithium reaction, while the ${}^3\text{He}$ is produced from the decay of tritium, ${}^3\text{H} \rightarrow {}^3\text{He}$ ($T_{1/2} = 12.38 \pm .03$ yr)⁵⁵. Normal isotope concentrations of ${}^6\text{Li}$ and ${}^{10}\text{B}$ are assumed throughout. These are 7.5% for ${}^6\text{Li}$ and 19.9% for ${}^{10}\text{B}$ ⁵⁶.

The samples were irradiated at two irradiation facilities. All the blood, plasma and protein samples were irradiated at the National Institute of Standards and Technology (NIST) reactor in Gaithersburg, Md. Samples of the various eluant components and Sephadex gel were irradiated at the McMaster reactor. Although the NIST reactor has a lower thermal neutron flux ($\sim 3.4 \times 10^{11} \text{ cm}^{-2} \text{ s}^{-1}$) at the irradiation position, compared to the sample irradiation position in the McMaster reactor ($\sim 10^{13} \text{ cm}^{-2} \text{ s}^{-1}$), it has the advantage of a much higher thermal/fast neutron ratio⁵⁷, which reduces fast neutron interference reactions to insignificant levels compared to the McMaster reactor. The most important fast neutron interference reactions are those on nitrogen, oxygen and carbon, all of which are major constituents of biological materials. These reactions are summarized in Table 2.1. Cross sections are average values taken from Cohen⁵⁸ and McLane et al.⁵⁹

Table 2.1

Interference Reactions

<u>Reaction</u>	<u>Neutron Energy</u>	<u>Target-nuclide cross section (mbarn)</u>	<u>Target-nuclide abundance⁵⁶ (%)</u>
$^2\text{H}(n,\gamma)^3\text{H}$	thermal	$.521 \pm .009^{60}$	0.015
$^{32}\text{S}(n,\alpha)^{29}\text{Si}$	thermal	3.9 ± 0.5^{61}	95.0
$^{33}\text{S}(n,\alpha)^{30}\text{Si}$	thermal	151 ± 22^{61}	0.75
$^{17}\text{O}(n,\alpha)^{14}\text{C}$	thermal	235 ± 5^{62}	0.038
$^{39}\text{K}(n,\alpha)^{36}\text{Cl}$	thermal	$0.10 \pm 0.05^*$	93.3
$^{35}\text{Cl}(n,\alpha)^{32}\text{P}$	thermal	0.08 ± 0.04^{60}	75.8
$^{40}\text{Ca}(n,\alpha)^{37}\text{Ar}$	thermal	2.4 ± 1.1^{63}	96.9
$^{14}\text{N}(n,^3\text{H})^{12}\text{C}$	>4.3 MeV	20	99.6
$^{12}\text{C}(n,\alpha)^9\text{Be}$	>6.3 MeV	100	98.9
$^{16}\text{O}(n,\alpha)^{13}\text{C}$	>2.4 MeV	100	99.8
$^{14}\text{N}(n,\alpha)^{11}\text{B}$	>0.2 MeV	100	96.9

Adapted from Clarke et al. (1987)¹³.

Fast neutron reactions are applicable only to the McMaster reactor.

*Author's estimate based on the irradiation of KCl. The published value of 4.3 ± 0.5 mbarn⁶¹ appears to be far too high (see Section 3.3).

The above-mentioned reactions can cause serious interference to lithium and boron measurements. In a previous experiment¹³ with whole blood samples irradiated at McMaster, it was shown that about 98% of the apparent lithium and 95% of the apparent boron were due to these fast neutron reactions. In contrast, results from a similar experiment¹³ indicated that fast neutron interference was less than 5% of apparent lithium and boron in whole blood in the sample irradiation position at NIST.

There are, however, a number of thermal neutron interference reactions which must be corrected for in both irradiation facilities. These include the neutron capture reaction ${}^2\text{H}(n,\gamma){}^3\text{H}$, which interferes with lithium measurements, and (n,α) reactions on sulfur, oxygen, potassium, chlorine and calcium, which interfere with boron measurements. A list of these is given in Table 2.1. The boron correction ΔB in ng/g dry weight is calculated for each type of sample, relative to the ${}^{10}\text{B}(n,\alpha){}^7\text{Li}$ reaction according to the formula

$$(\Delta B) = \sum_i \frac{C_i \sigma_i \lambda_i A_x}{\sigma_x \lambda_x A_i} \times 10^9 \text{ ng/g} \quad (2.1)$$

where C_i is the concentration of sulfur, oxygen, potassium, chlorine or calcium in the sample (see Table 2.2); σ_x and σ_i are the ${}^{10}\text{B}$ and target nuclide cross sections; λ_x and λ_i are the ${}^{10}\text{B}$ and target nuclide abundances; and A_x and A_i are the boron and target element atomic weights.

The samples irradiated at McMaster for the first experiment included NaCl, KCl, Na_2HPO_4 , KH_2PO_4 (all Gold Label grade), and Sephadex G-200 gel powder. These were irradiated for three hours in a core location with the aluminum holder continuously rotated during irradiation.

Table 2.2Concentration (g/g dry weight \pm 10%)

<u>Element</u>	<u>Blood</u>	<u>Plasma</u>	<u>Red Cells</u>	<u>Protein*</u>	<u>KCl</u>
H	.063	.060	.064	.0673	~ 0
O	.21	.18	.22	.23	~ 0
Cl	.013	.039	.0048	~ 0	.4755
K	.0078	.0018	.0099	~ 0	.5245
S	.0089	.0074	.0094	.0094	~ 0
Ca	.0003	.001	.00002	~ 0	~ 0

*Based on albumin

All values for blood, plasma and red cells are derived from data from wet weights given in Snyder et al.⁶⁴Thermal Corrections \pm 20%

<u>Material</u>	<u>(ΔB) ng/dry g</u>
Whole Blood	36
Plasma	32
Red Cells	38
Protein	38
KCl	29
PBS*	18

*phosphate-buffered saline

For the second experiment, samples of Gold Label and analytical grade KCl, analytical grade NaCl, and Sephadex G-200 were irradiated at McMaster for three hours in the same core position as before. An identical batch of samples was cadmium wrapped and irradiated the same way. Since cadmium ($\sigma_{th} = 20600$ barn for ^{113}Cd)⁶⁰ absorbs thermal neutrons but is transparent to epithermal and fast neutrons above 0.5 eV, an estimate of the fast neutron interference can be made.

Included in each holder were three blank liners and three standards. It was hoped that the blanks could be used to determine the localized increase in the fast neutron flux, occurring when the cadmium-wrapped container was lowered into the core position, through the threshold reaction $^{12}\text{C}(n,\alpha)^9\text{Be}$. This increase was noted in previous experiments by Clarke et al.¹³, and it is important to get an estimate of it in order to calculate the fast neutron interference more accurately. The standards were included to determine the cadmium ratio (R_{Cd}), which is defined as the ratio of activity in the bare sample to that in the cadmium wrapped samples. The samples were analyzed for ^3He and ^4He three weeks later in order to determine which grade of KCl was lowest in lithium and boron.

At NIST, three samples and one standard, or in some cases, two samples, one standard and one blank, were placed in a plastic container, which was sent by pneumatic tube to the irradiation position. The tubes were not rotated, so there were slight variations in the neutron flux reaching the samples. Each tube, or "rabbit", was irradiated for 24 hours, and then left to cool for at least 60 days to allow time for sufficient decay of ^3H to ^3He .

2.5 Mass Spectrometry

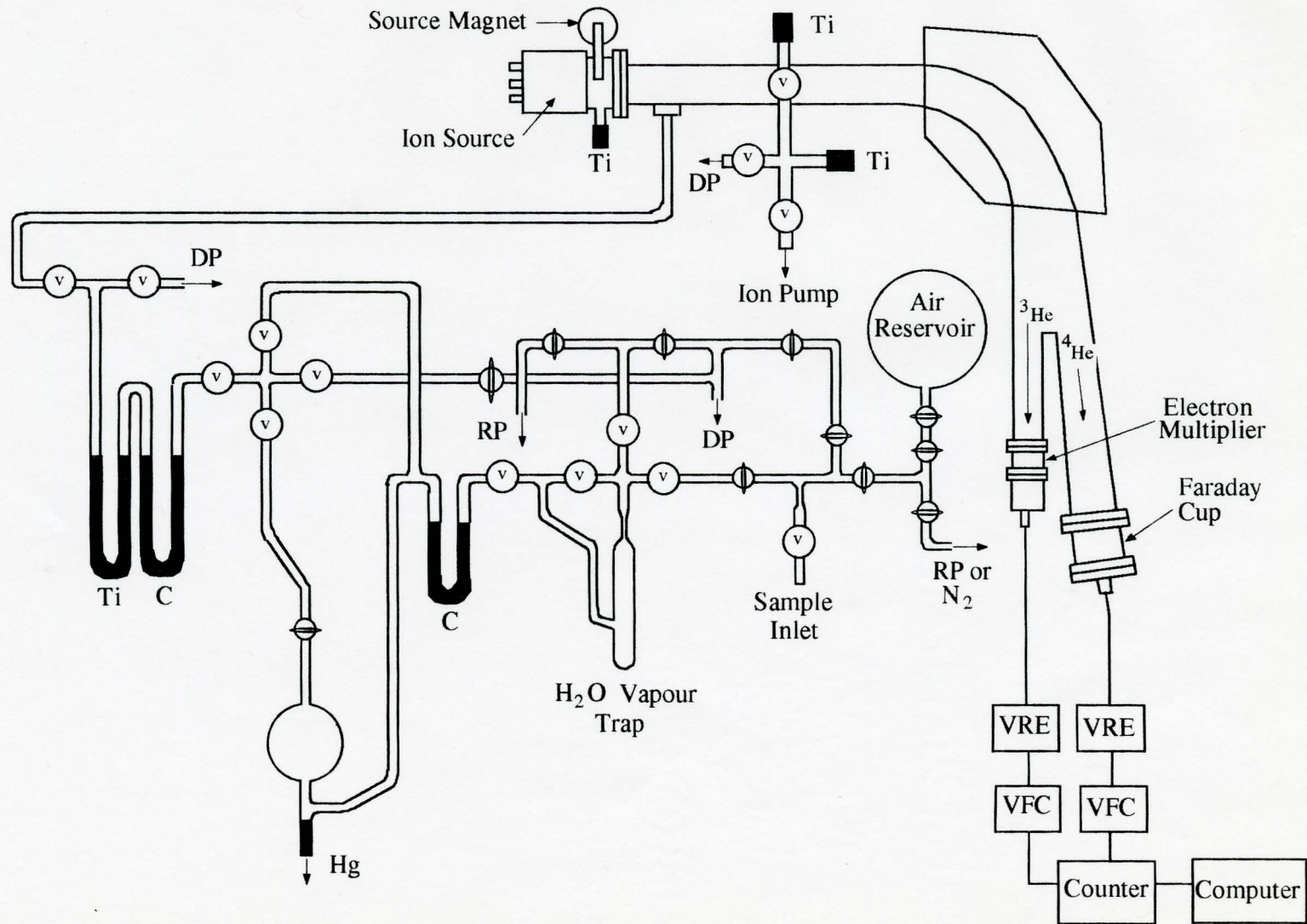
Analysis of ^3He and ^4He was carried out with a statically operated, dual collecting mass spectrometer, originally designed for oceanographic measurements

of helium isotopes and tritium in small water samples^{65,66} (see Figure 2.2). In static operation, the mass spectrometer is isolated from the pumps and a small sample is then introduced. The detection limits under good operating conditions are approximately 2×10^4 atoms of ^3He , and 2×10^{10} atoms of ^4He . The resolution is sufficient to clearly resolve the ^3He peak (^3He nuclidic mass = 3.016 amu) from the HD- H_3 peak (nuclidic masses = 3.022 amu and 3.023 amu respectively)⁵⁶.

Samples are introduced at the inlet to the processing line by puncturing the lead tube with a pin mounted on a modified bellows-type valve. The gas is purified before admission to the mass spectrometer by passing it through two liquid N_2 - cooled activated charcoal traps and then through titanium sponge to absorb hydrogen. Additional titanium sponges attached to the mass spectrometer volume served to decrease the HD- H_3 peak. The charcoal traps are heated between samples to release trapped gases, which are then pumped out.

The ^4He ion current is measured with a Faraday cup, while the ^3He is detected simultaneously with a Johnson-MM-1 electron multiplier. Data was acquired by means of two vibrating reed electrometers connected to a frequency counter through two voltage to frequency converters. The counter output, which is proportional to the ion current, was transferred to both a chart recorder and a computer. Computer analysis consisted of initial and final measurements of the ^4He peak and background, with ^3He peak height analysis in between. Background measurements for ^4He were obtained by increasing the accelerating voltage by 100 V, well off-peak. The ^3He analysis consisted of six background measurements at an accelerating voltage of 2847.6 V, with each of the background measurements followed by a set of integrations on the ^3He peak, at an accelerating voltage of 2843.6 V. The results were presented in both tabular and graphical form, with the

Figure 2.2. Mass spectrometer and processing line. Actual configuration is not exactly as shown. The processing line consists mainly of Corning 1720 glass and stainless steel. **v** = valve, **DP** = diffusion pump, **RP** = roughing pump, **Ti** = titanium metal sponge, **C** = activated charcoal, **VRE** = vibrating reed electrometer, **VFC** = voltage to frequency converter.



26a

^3He ion current extrapolated back to the time when the sample was introduced to the mass spectrometer inlet line. The average (weighted mean \pm 2 S.E.) ^3He ion current was also calculated for each sample. This was felt to be a more meaningful quantity, as the ^3He values normally showed no consistent trend from day to day.

Measurements of the ^3He and ^4He peak heights in the samples were made relative to the peak heights measured for known aliquots of air. Accordingly, at the beginning and end of each day's run, air aliquots were processed. Periodically throughout the day, mass spectrometer inlet line blanks were also measured. Included in the mass spectrometer line blank is any atmospheric He which diffuses into the glass portions of the instrument. The line blank ^4He showed a definite trend, which could be graphed. No such trend for the line blank ^3He was discernible; instead, a weighted mean \pm S.E. was calculated from the average line blank ^3He . Data from the mass spectrometric analysis was then used to calculate lithium and boron in the samples.

2.6 Gamma Counting

Since the rabbits holding the samples during the NIST irradiations were not rotated, one may expect small variations in the neutron flux reaching each sample in the holder, as mentioned earlier. The flux is estimated from the standard in each rabbit by calculating the flux necessary to give a lithium reading of 52.45 ng/g wet weight. The boron measurement is less reliable, apparently because the boron compound is more volatile, and some is lost at some stage in the experiment.

The relative neutron flux reaching the other samples, normalized to the standard, is estimated by gamma-counting of the lead tubes. The decay of the

isotope ^{124}Sb ($T_{1/2} = 60.2$ days, photopeak = .603 MeV)⁶⁷, produced by the reaction $^{123}\text{Sb}(n,\gamma)^{124}\text{Sb}$ in the lead tubes, is convenient for gamma-counting.

From each lead tube, a piece 2.15 cm long was cut from the portion enclosing the sample. After weighing the pieces, gamma-counting was carried out with a multichannel analyzer operating in PHA mode, and an NaI (Tl) scintillation counter. Each tube was analyzed by rotating it one-quarter turn after each count (~ 30 sec.), and then averaging the four results. With the standard normalized to 1.0000, the relative neutron flux to the other three samples was determined. The flux variation for four samples in a rabbit was typically < 6%.

Chapter 3

Results and Discussion

3.1 Introduction

In this chapter, the results of the two gel filtration experiments are discussed. Most of the emphasis will be on the data from the second experiment, although the results of the first experiment are mentioned by way of comparison. Of the two experiments, the second was more conclusive with regard to lithium binding to the proteins in the gel column fractions. The lithium data from the first experiment were less clear. Still, many of the same features observed in the second experiment could be seen here, although they were somewhat obscured by the high lithium background from the phosphate-buffered saline used as the eluant. The similarities between the two boron profiles are more obvious, as shown by a comparison of Figures 3.4(a) and 3.5(a). Although the boron background in the first experiment was considerably higher than in the second experiment, the boron profile was not obscured to the same extent as the corresponding lithium profile. Before going on to the actual discussion of the binding of lithium and boron to proteins, a number of other topics relevant to the experiments will be considered. These include a summary of the equations used to translate the mass spectrometer data into ng of lithium and boron in the samples; an observation concerning the reaction cross section for the thermal neutron reaction $^{39}\text{K}(n,\alpha)^{36}\text{Cl}$, one of the reactions listed in Table 2.1; and the lithium and boron contents of whole blood, plasma and red blood cells, with reference to other published results.

3.2 Interpretation of Mass Spectrometer Data

Before a detailed analysis of the lithium and boron content of the samples can begin, it is necessary to translate the mass spectrometer data, given in mV, into atoms of ^4He , and atoms of ^3He (and hence to atoms of tritium), and then into ng of lithium and boron.

The total number of ^4He atoms in a sample is given by the following equation:

$$^4\text{He atoms} = \frac{(^4\text{He}_s - ^4\text{He}_b)}{(^4\text{He}_a - ^4\text{He}_b)} \times A_0 \times (f)^n \quad (3.1)$$

Similarly, the number of ^3He atoms is given by:

$$^3\text{He atoms} = \frac{(^3\text{He}_s - ^3\text{He}_b)}{(^3\text{He}_a - ^3\text{He}_b)} \times A_0 \times (f)^n \times R \quad (3.2)$$

where,

$^4\text{He}_s$ and $^3\text{He}_s$ are the observed peak heights (mV) in the sample

$^4\text{He}_b$ and $^3\text{He}_b$ are the peak heights (mV) of the mass spectrometer line blanks. $^3\text{He}_b$ is the weighted average (mV) of all the line blanks processed on a given day.

$^4\text{He}_a$ and $^3\text{He}_a$ are the peak heights (mV) observed in the air aliquot

A_0 is the amount of ^4He in the standard air aliquot, expressed in atoms at STP

f is a depletion factor for the ^4He in the air aliquot

n is the air aliquot number

R is the atmospheric $^3\text{He}/^4\text{He}$ ratio, taken to be 1.384×10^{-6} , as determined previously by Clarke et al.^{65,68}

The total tritium in the sample is then calculated from the number of ^3He atoms by the following relation:

$$^3\text{H atoms} = \frac{^3\text{He}}{(1 - e^{-\lambda t})} \quad (3.3)$$

where,

^3He is the number of ^3He atoms from Eq. (3.2)

λ is the decay constant in days^{-1}

t is the decay time in days, counted from the mid-point of the irradiation

^3H must then be corrected for initial sample tritium (i.e. environmental tritium), liner tritium, and tritium produced by the interference reaction $^2\text{H}(n,\gamma)^3\text{H}$. The first two corrections are determined from the non-irradiated samples and blanks respectively, while the third is determined by:

$$(H \times \text{dry wt} + .143 \times \text{liner wt}) \times \frac{N_A}{A_x} C_i \sigma_i \Phi t \quad (3.4)$$

expressed as ^3H atoms, where,

H is the concentration of H in the sample (g/g)

dry wt is the dry sample mass in g

.143 is the concentration of H in the polyethylene liner material (g/g)

liner wt is the liner mass in g

N_A is Avogadro's number

A_x is the atomic weight of H

C_i is the concentration of ^2H from Table 2.1, expressed as a decimal percentage

σ_i is the reaction cross section from Table 2.1 in 10^{-24} cm^2

Φ is the thermal neutron flux in $\text{cm}^{-2}\text{s}^{-1}$

t is the irradiation time in seconds

Corrections to the total ^4He calculated from Eq. (3.1) include the ^4He from non-irradiated samples, the average ^4He from the irradiated blanks, and ^4He from the $^6\text{Li}(n,^3\text{H})^4\text{He}$ reaction.

From the corrected values for ^3H and ^4He , the lithium and boron content of the samples in ng is calculated from the following relations:

$$\text{Li (ng)} = ^3\text{H} \times \frac{A_x}{N_A \Phi \lambda_x \sigma_x t} \times 10^9 \text{ ng/g} \quad (3.5)$$

where,

A_x is the atomic weight of lithium (g/mole)

λ_x is the abundance of ^6Li (decimal percentage)

σ_x is the $^6\text{Li}(n,^3\text{H})^4\text{He}$ reaction cross section in 10^{-24} cm^2

Φ , t as in Eq. (3.4)

$$\text{B (ng)} = ^4\text{He} \times \frac{A_x}{N_A \Phi \lambda_x \sigma_x t} \times 10^9 \text{ ng/g} \quad (3.6)$$

where this time,

A_x is the atomic weight of boron (g/mole)

λ_x is the abundance of ^{10}B (decimal percentage)

σ_x is the $^{10}\text{B}(n,\alpha)^7\text{Li}$ reaction cross section in 10^{-24} cm^2

Φ , t as before

In addition, the thermal (n,α) correction, ΔB , calculated for the particular sample, must be subtracted from the boron value obtained from Eq. (3.6):

$$\text{Corrected B (ng)} = \text{B (ng)} - \Delta\text{B (ng/g)} \times \text{dry sample wt (g)} \quad (3.7)$$

Lithium and boron in each sample can then be expressed in ng/g wet weight or ng/g dry weight by dividing by the wet or dry weight in g.

3.3 Thermal $^{39}\text{K}(n,\alpha)^{36}\text{Cl}$ Cross Section

After the results from the McMaster irradiations done prior to the second gel filtration experiment were analyzed, it was observed that the thermal (n,α) correction previously calculated for KCl appeared to be far too large. This led to speculation that the published value of 4.3 ± 0.5 mbarn⁶¹ for the thermal reaction $^{39}\text{K}(n,\alpha)^{36}\text{Cl}$ might be in error. As the contribution to the total correction from chlorine, calculated from Eq. 2.1, was very small compared to the potassium correction, a significant overestimation of the potassium cross section was considered more likely.

As mentioned earlier, two sets of samples, one cadmium-wrapped, and the other unwrapped, were irradiated at McMaster. Included in these samples were a number of blanks. By comparing the average number of ^4He atoms, produced by the fast neutron reaction $^{12}\text{C}(n,\alpha)^9\text{Be}$ on the liner material, the difference in fast neutron flux to the cadmium-wrapped samples and the unwrapped samples could be estimated. The liner material is known to contain almost no boron¹³, so within experimental error, all of the increase in ^4He in the cadmium-wrapped blanks compared to the unwrapped blanks should be due to a greater fast neutron flux.

After adjusting the flux to the cadmium-wrapped samples, the apparent boron in the two sets of samples was compared. From this comparison, it was estimated that about 96% of the apparent boron in KCl was due to fast neutron (n,α) reactions on both potassium and chlorine. Although both these reactions are possible at thermal energies (see Table 2.1), they have maximum cross sections of about 150 mbarn for potassium, and about 110 mbarn for chlorine at approximately 7 - 8 MeV⁵⁸. Thus, fast neutron reactions would predominate. The remaining apparent boron in the analytical grade KCl, after correcting for fast

neutron reactions, averaged 36 ng/g of dry KCl. Based on the published value for the potassium cross section, the thermal correction should have been 773.3 ng/g, of which 11.5 ng/g would have come from chlorine, and 761.9 ng/g from potassium. Clearly, this estimate was too high, since it would have resulted in very large negative boron values for KCl after applying the thermal correction. Therefore, a new estimate was made using the data from the gel column fractions eluted with KCl, and irradiated at NIST, where fast neutron interference is negligible.

In making this estimate, the column fractions with the lowest apparent boron content were chosen, and a thermal correction applied which forced these boron values to zero, within experimental error. Since it is possible to have no boron in a sample, but not "negative" boron, it was determined that a maximum thermal correction of 29 ng/g was more appropriate for KCl. This left 7 ng/g as the estimated actual boron content of the analytical grade KCl. Assuming the $^{35}\text{Cl}(n,\alpha)^{32}\text{P}$ cross section is essentially correct, application of Eq. (2.1) results in a new value of ~ 0.10 mbarn for the thermal neutron reaction on potassium. Thus, as noted in Table 2.1, a cross section of 0.10 ± 0.05 mbarn was used in all thermal (n,α) corrections involving potassium.

3.4 Lithium and Boron in Whole Blood and Components

Four sets of samples of whole blood, plasma and red blood cells were analyzed for lithium and boron content. Three sets were from "Donor A", whose plasma was used in both gel filtration experiments, and one set was from a second donor, "Donor B". The most important information obtained from these samples was the lithium and boron content of the plasma applied to the gel column. This information allowed the calculation of the total expected lithium and boron in the

protein fractions. Lithium and boron in the whole blood and component samples are summarized in Table 3.1.

The results presented in Table 3.1 are the weighted averages \pm one standard error of the mean, of at least two, and sometimes three samples each of whole blood, plasma and red cells from each donor, with the red cell lithium and boron corrected for interstitial plasma. This correction is necessary because not all the plasma is separated from the red cells during centrifuging. Since lithium levels in plasma are normally much higher than in red cells, the interstitial plasma can add significantly to the apparent lithium in the red cell fraction. The boron contribution from plasma is smaller, but can still result in a correction of several ng/g. Estimates of the percentage of trapped plasma were made by comparing the experimental red cell wet-to-dry weight ratios with a standard ratio of 2.67 derived from Snyder et al.⁶⁴ The estimated interstitial plasma ranged from 8.2% to 15.5% of red cell mass.

Also included in Table 3.1 are the lithium and boron ratios for each set of samples. The lithium (boron) ratio is defined as the ratio of red cell lithium (boron) to plasma lithium (boron). In this work, these ratios were calculated in terms of lithium (boron) in red cell water versus lithium (boron) in plasma water, where red cell water (g) = (red cell wet weight - red cell dry weight) in g, and plasma water (g) = (plasma wet weight - plasma dry weight) in g. The red cell and plasma lithium and boron values in ng/g wet weight can be expressed in terms of red cell and plasma water by multiplying the red cell values by about 1.6 and the plasma values by about 1.1.

Results for whole blood summarized in Table 3.1 are in good agreement with values reported elsewhere by Clarke et al.^{12,13}, but are lower than other results mentioned earlier^{11,14,15,46}. There is also good agreement in the lithium

Table 3.1 (a)

Lithium in Whole Blood and Components

<u>Donor</u>	<u>Date</u>	<u>Component</u>	<u>ng/g dry wt</u>	<u>ng/g wet wt</u>	<u>Li Ratio</u>
A(1)	1/89	Whole Blood	1.90 ± .10	.40 ± .02	.27 ± .05
		Plasma	6.07 ± .29	.55 ± .03	
		Red Cells	.27 ± .05	.10 ± .02	
B	1/89	Whole Blood	1.75 ± .10	.38 ± .03	.23 ± .05
		Plasma	7.51 ± .23	.69 ± .02	
		Red Cells	.29 ± .05	.11 ± .02	
A	12/89	Whole Blood	2.54 ± .10	.53 ± .02	.33 ± .05
		Plasma	6.88 ± .16	.66 ± .01	
		Red Cells	.41 ± .06	.15 ± .02	
A(2)	1/90	Whole Blood	2.24 ± .08	.47 ± .01	.32 ± .04
		Plasma	6.35 ± .12	.60 ± .01	
		Red Cells	.35 ± .02	.13 ± .02	

Table 3.1 (b)

Boron in Whole Blood and Components

<u>Donor</u>	<u>Date</u>	<u>Component</u>	<u>ng/g dry wt</u>	<u>ng/g wet wt</u>	<u>B Ratio</u>
A(1)	1/89	Whole Blood	150 ± 7	31.3 ± 1.4	.98 ± .10
		Plasma	382 ± 9	34.1 ± 0.8	
		Red Cells	61 ± 6	22.9 ± 2.4	
B	1/89	Whole Blood	91 ± 7	19.6 ± 1.4	.68 ± .14
		Plasma	261 ± 8	23.8 ± 0.7	
		Red Cells	29 ± 6	11.0 ± 2.3	
A	12/89	Whole Blood	158 ± 7	33.5 ± 1.5	.96 ± .08
		Plasma	356 ± 9	33.9 ± 0.8	
		Red Cells	61 ± 5	22.6 ± 1.9	
A(2)	1/90	Whole Blood	115 ± 5	23.9 ± 1.1	1.09 ± .09
		Plasma	307 ± 6	28.3 ± 0.6	
		Red Cells	57 ± 5	21.4 ± 1.7	

(1) = Gel Filtration Experiment #1; (2) = Gel Filtration Experiment #2

All red cell values corrected for interstitial plasma.

Li and B ratios are calculated as Li (B) in red cell *water* / Li (B) in plasma *water*.

and boron concentrations in the samples from Donor A taken one year apart, which suggests that these concentrations remain fairly constant in an individual over time.

The lithium ratios were all <1.0 , which is consistent with the fact that Li^+ is transported out of red cells against its concentration gradient by a $\text{Na}^+\text{-Li}^+$ countertransport mechanism⁶⁹. In all samples from Donor A, the lithium ratios remained the same (within experimental error) over a period of one year, as did the boron ratios. Boron ratios, at least from Donor A, seemed to indicate that boron was equally distributed between red cell water and plasma water, suggesting that no active transport mechanism, analogous to that for lithium, exists for boron. The boron ratio for Donor B does not show this characteristic, but with such a small number of donors, no definite conclusion about boron transport can be made.

3.5 Protein Separations: Protein Profiles

After freeze-drying was completed, the protein content of each column fraction was calculated. As a first step, a plot of $(\text{dry wt/wet wt}) \times 1000$, or $(D/W) \times 1000$, vs. total fluid in g was made to determine the distribution of the protein peaks. The first several fractions before the protein peaks, and the remaining fractions after the peaks were taken to represent the eluant background. The background wet-to-dry weight ratios (W/D ratios) for the fractions in the protein peaks were interpolated from a linear least squares fit, $y = mx + b$, where y is the calculated eluant W/D ratio for a fraction, x is total fluid in g, and m and b are the slope and intercept respectively, calculated by the method of least squares. From these interpolated values for the eluant W/D ratios, the amount of dry eluant material in each fraction in the protein peaks could be determined. Using KCl as an example, this amount was calculated as follows:

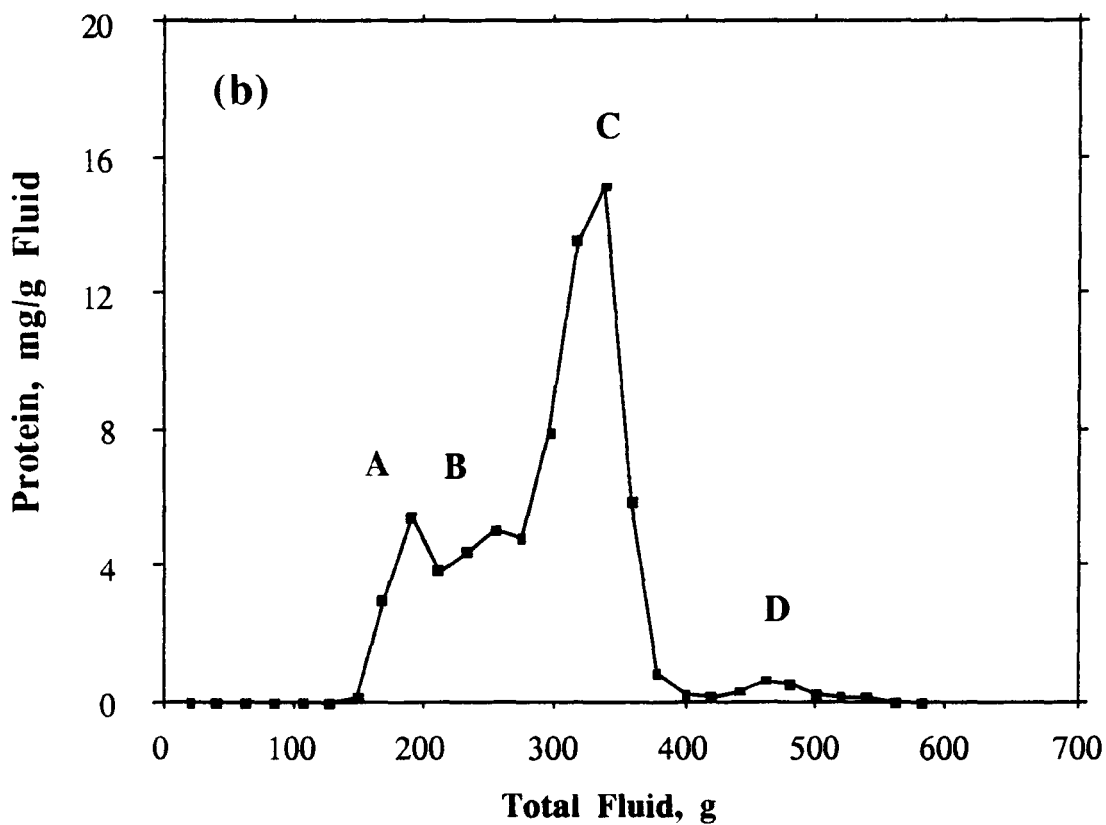
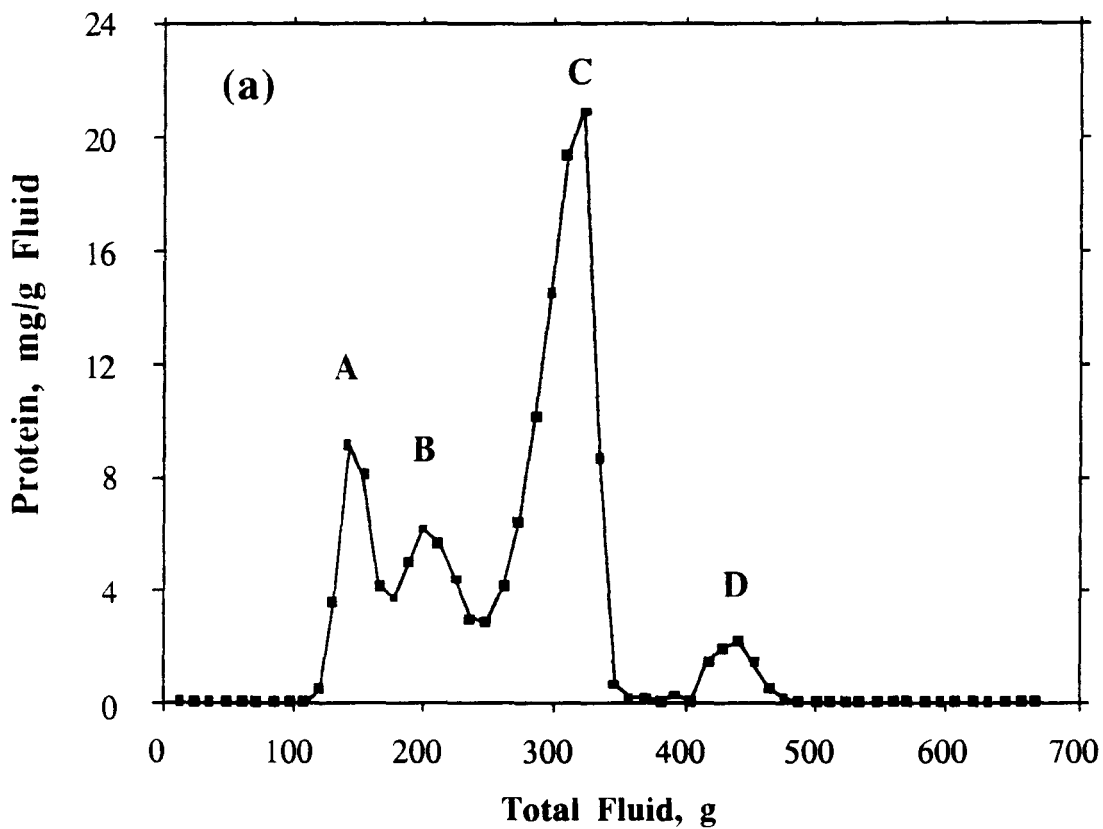
Figure 3.1. Protein profiles, plotted as mg of protein/g of fluid in each fraction vs. total fluid (g) collected.

(a) Gel Filtration Experiment #2. Letters identify the different protein peaks:

A = high molecular weight proteins largely excluded from the gel; **B** = medium weight proteins; **C** = albumin peak; **D** = "ion" peak.

(b) Gel Filtration Experiment #1. Letters mark the location of the peaks in (a) in relation to those in (b).

38a



$$\frac{\text{KCl} + \text{H}_2\text{O}}{\text{KCl}} = \frac{W}{D} \text{ (of KCl)} \quad (3.8)$$

so that,

$$\text{KCl} = \frac{\text{H}_2\text{O}}{(W/D) - 1} \quad (3.9)$$

where KCl (g) = dry weight of KCl in g, and H₂O (g) = (sample wet wt - sample dry wt) in g. The amount of protein in a fraction was the difference between the total sample dry weight and the calculated eluant dry weight.

With this information, mg of protein/g of fluid in each fraction was plotted against total fluid in g. Plots for the two gel filtration experiments are shown in Figure 3.1. Figure 3.1(a) shows the protein profile from the second protein separation experiment, while Figure 3.1(b) is the protein profile from the first experiment. The letters A,B,C,D in Figure 3.1(a) mark the location of the three protein peaks, and the ion peak respectively. These same letters are used in Figure 3.1(b) to show how the positions of the peaks eluted in the first separation relate to those from the second separation. A comparison of the two plots shows that the maxima of the first two peaks do not coincide, although the third peak and ion peak coincide quite well. This may simply reflect the difference in fraction size between the two experiments. The resolution in 3.1(a) is also considerably improved as a result of taking a larger number of smaller fractions. However, total elution volume, that is, the volume required to elute the contents of all four peaks, was essentially the same for both protein separations.

Proteins are eluted approximately in order of decreasing molecular weight, although there are some proteins which, because of their shape, do not follow this pattern exactly. In the ion peak, some of what is labelled "protein" actually consists of sugars and ions instead, since plasma normally contains 0.95% (wet

Table 3.2

Some Representative Plasma Proteins

<u>Protein</u>	<u>Peak Location</u>	<u>Molecular Wt (amu)</u>	<u>Average Abundance (mg/100 ml plasma)</u>
VLDL*	A	$5 \times 10^6 - 20 \times 10^6$	200
β -lipoprotein	A	$2 \times 10^6 - 2.7 \times 10^6$	350
IgM**	A	950 000	155
α_2 -macroglobulin	A	725 000	285
haptoglobin 2-2	trough between A and B	400 000	190
α_1 -lipoprotein	trough between A and B	375 000	325
haptoglobin 2-1	B	200 000	230
IgA	B	160 000	270
IgG	B	150 000	1300
ceruloplasmin	B	132 000	38
haptoglobin 1-1	trough between B and C	86 000	160
transferrin	trough between B and C	79 500	260
albumin	C	66 500	4250
α_1 -antitrypsin	C	54 000	300
β_2 -glycoprotein I	C	48 000	23
α_1 acid glycoprotein	C	40 000	98

*Very Low Density Lipoproteins

**Ig = immunoglobulin

Information on lipoproteins from Scott et al.⁷⁰

Information on all other proteins from Putnam⁷¹.

weight) ions, and about 0.1% (wet weight) glucose⁶⁴. Referring to Figure 3.1(a), Peak A contains the high molecular weight proteins (> 600 000 amu) which are largely excluded from the gel pores. Peak B contains medium weight proteins, mainly IgG (immunoglobulin G), Peak C consists mostly of albumin, the most abundant plasma protein, and Peak D, as previously mentioned, contains sugars, other small molecules (< 5000 amu) and ions. Table 3.2 lists some representative plasma proteins from the protein peaks A, B and C, along with their molecular weights and average abundance. Molecular weights of many proteins are not precisely known, so the stated values may vary from one reference to another.

3.6 Protein Separations: Lithium and Boron Profiles

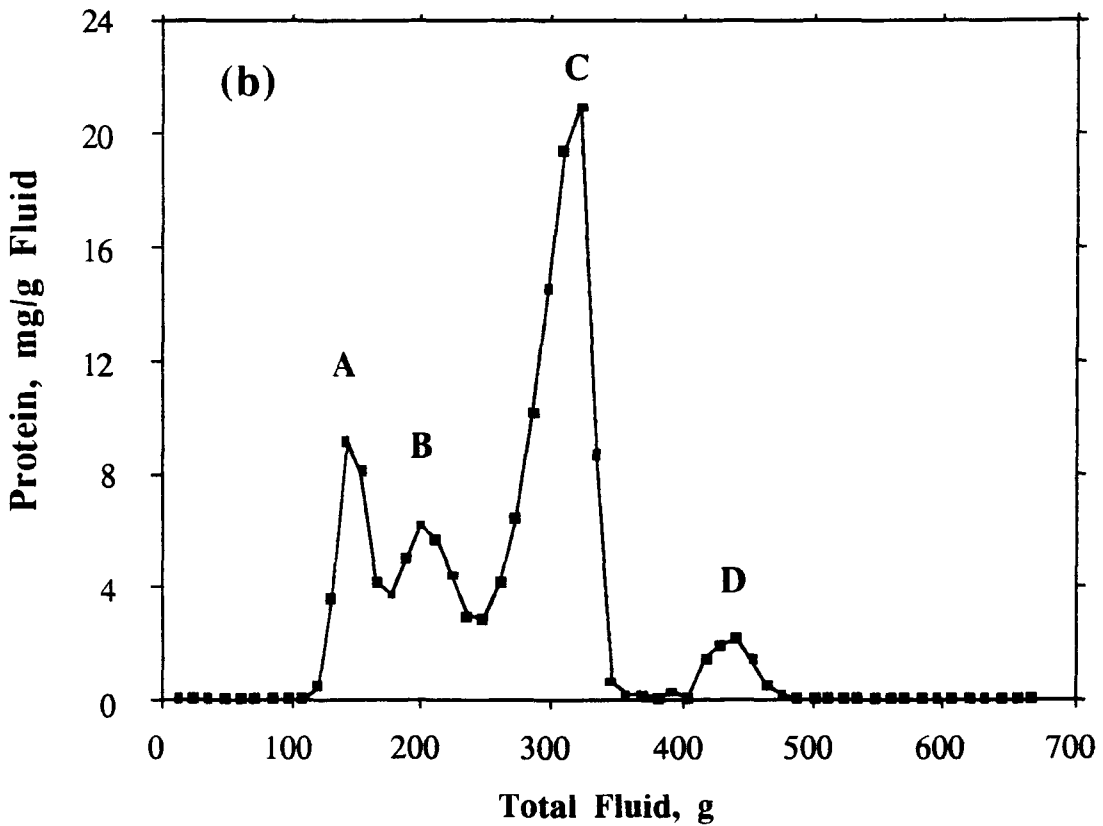
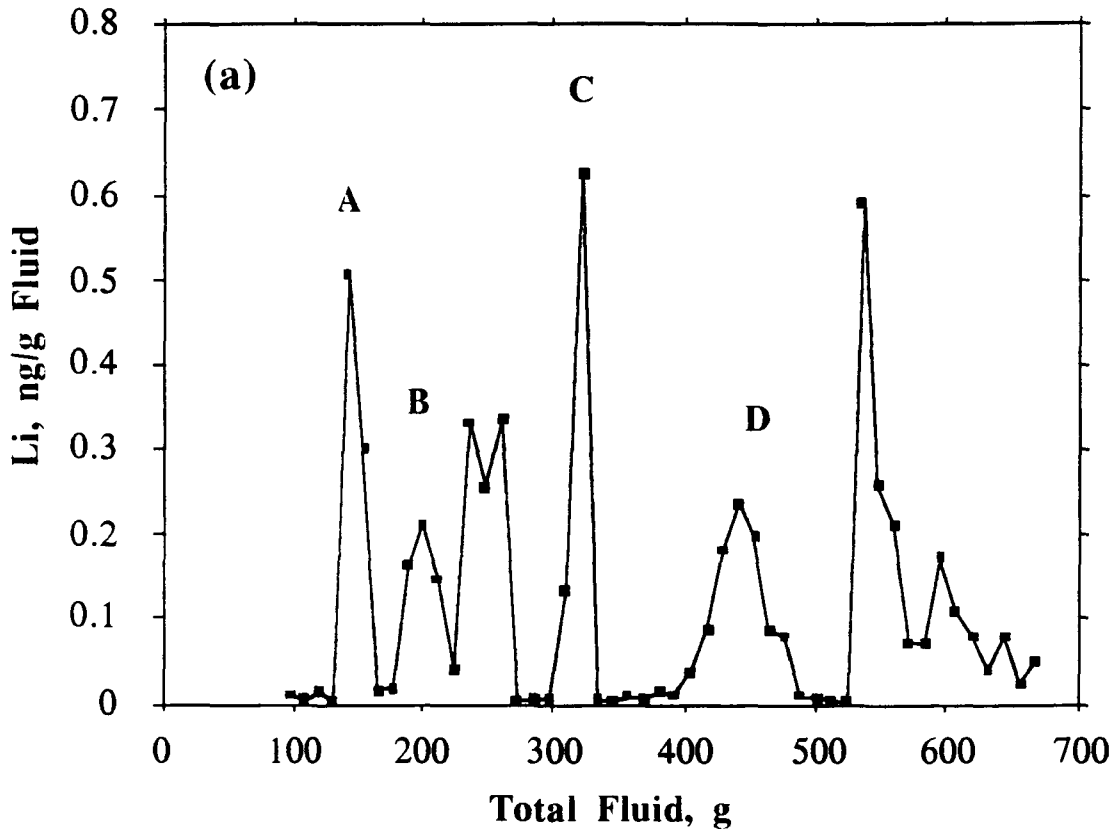
As noted at the beginning of this chapter, only the results of the second gel filtration experiment will be treated in detail. Therefore, all discussion in this section, unless otherwise stated, refers to the second experiment. Lithium distribution in the gel column fractions will be discussed first, followed by the boron distribution.

Analysis of the mass spectrometer ³He data revealed an initial series of five lithium peaks associated with the protein fractions (including the ion peak), plus another series of lithium peaks which followed after the end of the ion peak (Peak D in Figure 3.1(a)). The lithium profile formed by three of the five initial peaks closely matches the protein profile, both in relative size and position, coinciding as it does with protein peaks A, B and C. A fourth lithium peak coincides with the trough between peaks B and C. This peak actually appears to consist of two peaks which are not completely resolved, and is perhaps the most interesting feature in the lithium profile, for reasons which will be discussed later. The maximum of the

Figure 3.2. (a) Lithium Profile for Gel Filtration Experiment #2, where ng Li/g of fluid in each fraction are plotted vs. total fluid (g). The KCL background is included. Letters mark the positions of the protein peaks. Lithium peaks beyond **D** are replacement peaks.

(b) Protein profile for Gel Filtration Experiment #2.

42a



fifth lithium peak coincides approximately with the maximum of protein peak D, although the peak itself extends into the region between peaks C and D, a region of low molecular weight proteins. At the trailing edge of this lithium peak is what appears to be another, smaller peak only partially resolved. This area, which contains an estimated 1.8 ng of lithium, may be the actual Li^+ ion peak. The remainder of the fifth peak may contain lithium associated with sugars and other small organic molecules.

A plot of the lithium profile is shown in Figure 3.2(a), with ng of lithium/g of fluid in each fraction plotted against total fluid (g) eluted. The quantity ng of lithium/g of fluid was calculated by first determining the total lithium content of each fraction from the mass spectrometer data, and then dividing by the total fluid (g) in the fraction. The values plotted in Figure 3.2(a) include the KCl lithium background of 0.008 ng/g of solution (1.36 ng/g of dry KCl). These results clearly indicate that lithium can bind to plasma proteins to a considerable extent, at least *in vitro*. This is in contradiction to the assertion that lithium does not bind to plasma proteins.^{10,41-44}

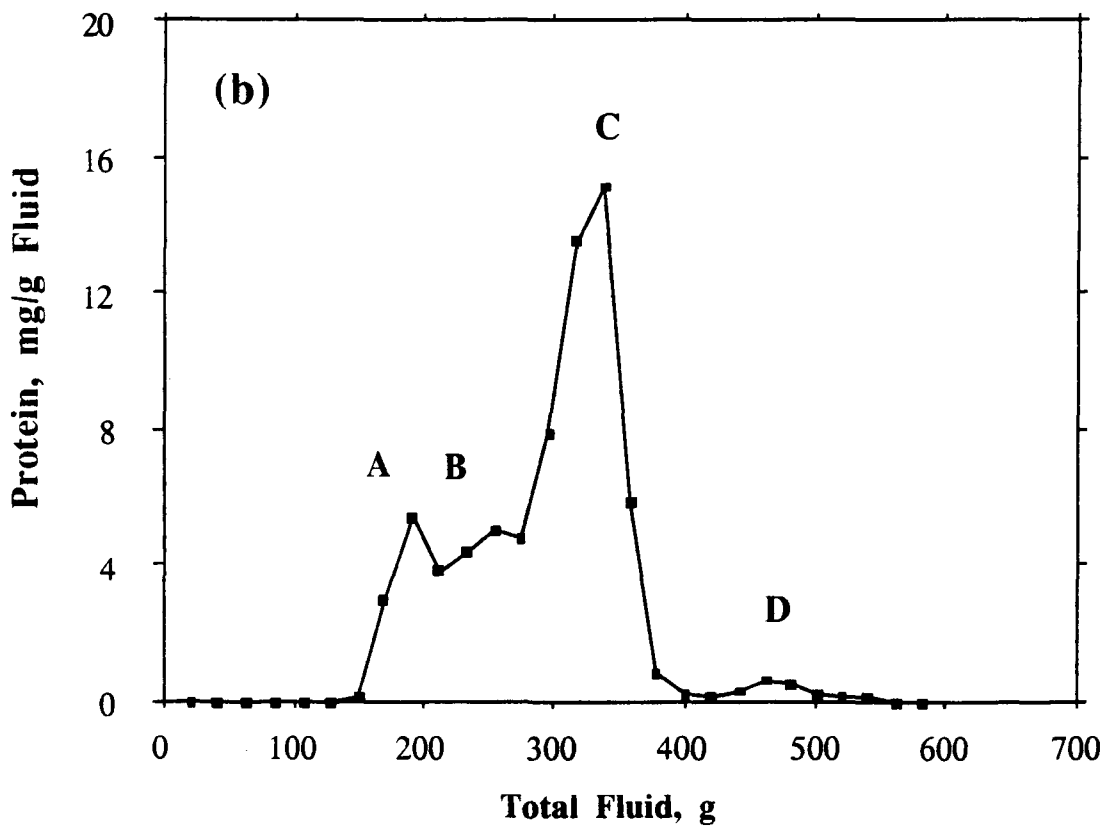
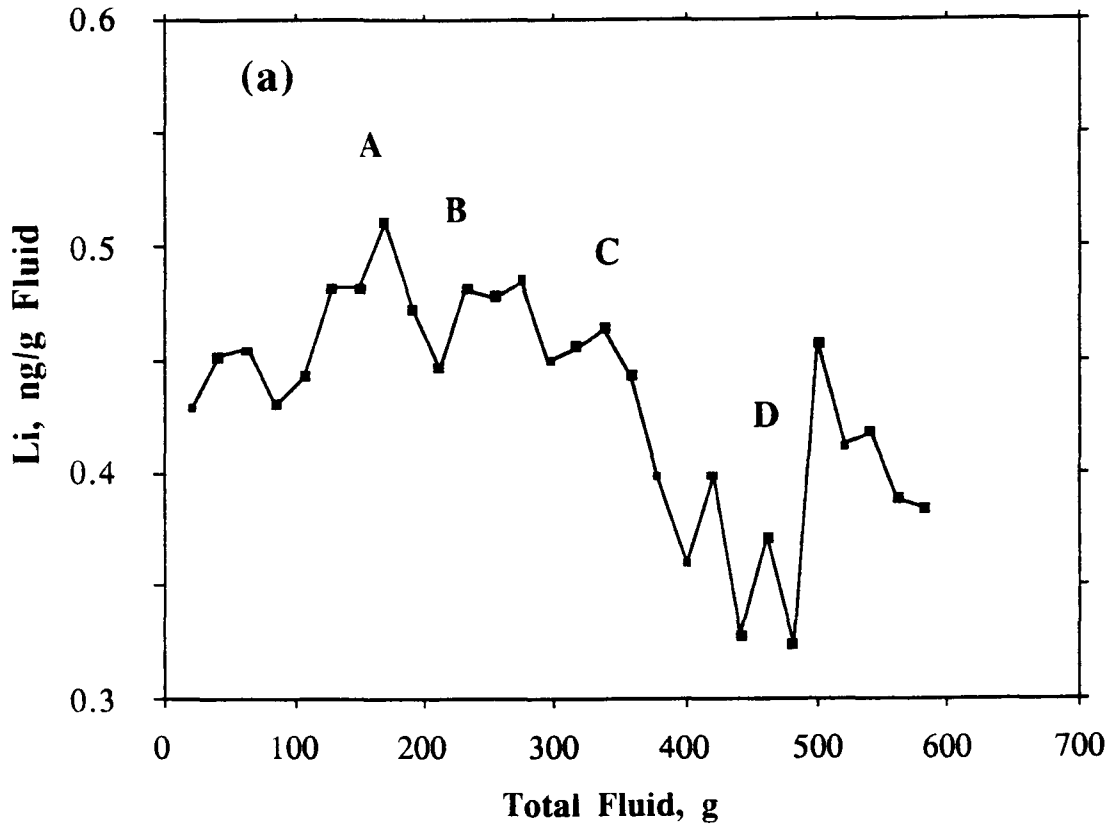
A similar plot of the lithium profile from the first gel filtration experiment is shown in Figure 3.3(a). Most of the same features observable in Figure 3.2(a) can be seen here, but they are nearly overwhelmed by the high lithium background of the PBS eluant, calculated to be 33.6 ng/g of the dry mixture, or 0.313 ng/g of PBS solution. The double lithium peak between B and C, seen in figure 3.2(a), appears in 3.3(a) as only one peak.

The series of lithium peaks which follow after peak D (Figure 3.2(a)) were puzzling at first, since they did not seem to be related in any way to the plasma proteins. However, a likely explanation is that these are replacement peaks, caused by certain cations, such as K^+ , Ca^{+2} , Na^+ , and Mg^{+2} , which are present in plasma,

Figure 3.3. (a) Lithium profile for Gel Filtration Experiment #1. PBS background is included. Letters mark the positions of the protein peaks from Experiment #2 (see Figure 3.2 (b)). A replacement peak is visible beyond D.

(b) Protein profile for Gel Filtration Experiment #1. Letters mark positions of the protein peaks from Experiment #2 relative to those in this figure.

44a



and in the case of K^+ , also in the eluant, displacing Li^+ from the gel. A similar effect of these same cations on Zn^{+2} was observed by Evans et al.⁵² Apparently the gel acts as a kind of ion exchange column, in which the cations listed above successively displace Li^+ in order of decreasing ionic radius, where the radius of $K^+ > Ca^{+2} > Na^+ > Mg^{+2}$. Thus, the elution volume of a particular replacement peak is inversely related to the ionic radius of the cation which displaces the Li^+ . It is unclear whether these other cations remain in the gel, or are subsequently eluted. Based on concentrations of ions given in Snyder et al.⁶⁴, the mass of these four ions, plus Cl^- and Br^- should be about 150 mg for the amount of plasma added to the column. The calculated "protein" in the ion peak is estimated at 96 mg, so it appears that not all the ions were recovered, although it is difficult to believe that the gel could retain 50 or more mg of ions. It is more likely that the estimate of 150 mg for the total ion mass is too high.

Returning to the lithium peaks associated with the protein fractions, an examination of the lithium distribution of peak A shows that most of the lithium is spread out over the central area of the peak, dropping sharply near the leading edge, and in the trough between peaks A and B. In these latter two regions, the lithium concentration drops close to the lithium background concentration for the KCl, or even below, indicating that in some fractions, the eluant has been depleted in lithium. The lithium distributions in peak B, and in the region between B and C have similar widths, and like the lithium peak in A, drop to background at their edges, but the lithium peak corresponding to peak C is very sharp, rising and falling over only two fractions. In peak D, the lithium is spread out over much of the low molecular weight range, with the concentration dropping sharply on either side of the peak.

The lithium distribution observed in peaks A and B suggests at first that most of the proteins in each peak are binding lithium, i.e. it is a non-specific type of binding. However, the shape of the peaks may be misleading, even though they cover most of their respective protein peaks. Other works^{28,34,50,72} dealing with the binding of metal ions to proteins show the shape of the metal ion peaks to be variable. These were all studies of ions such as Cu^{+2} , Zn^{+2} and Fe^{+3} which are known to bind to specific proteins, yet the metal peaks in the illustrations were sometimes broad and symmetric, covering most of the protein peak^{34,72}, and sometimes sharp and either symmetric or asymmetric^{28,50}. In all cases, only one protein in a peak was involved. Therefore, although the lithium peaks in our results are variable in shape, it seems more likely that only one protein in each of peaks A and B is involved in lithium binding. Specific binding sites are further suggested by the fact that there are clear divisions between the lithium peaks. This same type of specific binding to a single protein is probably the case in peak C as well. In peak D, the situation is less clear, although there could be binding to a small number of low molecular weight substances. Finally, the lithium peak between B and C is interesting because it is not associated with a protein peak, and so should contain only a small number of proteins. The fact that there are apparently two partially resolved peaks here may mean that two distinct proteins are binding lithium.

Whether the pattern of lithium binding described above exists *in vivo* is uncertain. Instead, it could be the result of the proteins "scavenging" traces of lithium from the gel. The scavenging hypothesis was originally formulated by Evans and Fritze⁷² to explain the appearance of "extra" metal ion peaks in protein fractions. In their study of the distribution of copper in plasma proteins using gel filtration, they observed a second copper peak in the region corresponding to peak

A, when only one copper peak, that of copper bound to ceruloplasmin in peak B, was expected. They attributed this extra peak to scavenging of copper from the gel by a high molecular weight protein. This second peak was eliminated by washing the gel to remove residual copper before adding the serum sample to the gel column. In a more recent series of experiments, Gardiner et al.²⁸ reported the appearance of a higher proportion of zinc than expected, along with extra iron and copper peaks in the high molecular weight protein peak, which they could not explain in terms of a specific interaction with a protein. The calculated total metal recovered from the column for each element was more than 200% of the starting amount. They concluded that the excess zinc, iron and copper were coming from the gel, and indeed found that the gel (Sephadex G-150) contained significant amounts of all three metals. The extra peaks were eliminated by removing trace metals from the gel and the eluant prior to adding the serum. The report is somewhat vague about whether more than one protein was believed to be involved in picking up the extra metal ions.

The case for scavenging of lithium by proteins is made more plausible by the fact that a mass balance for lithium indicated substantially more lithium than would be expected from the plasma in both gel filtration experiments. The details of this mass balance are given in Table 3.3. An interesting feature to note is that after the eluant background is subtracted out, the total amounts of lithium recovered in both experiments are very similar, despite the much higher lithium content of the PBS eluant compared with the KCl eluant. Even including the eluant lithium, the total recovered in experiment #1 is only 3.65 times higher than that in experiment #2, yet the PBS contains about 39 times the lithium of the KCl per g of solution.

The question then arises as to the source of the excess lithium. Gardiner et al.²⁸ concluded that the excess metals in their column fractions were coming from

Table 3.3

Total Lithium and Boron in Plasma Protein Fractions

<u>Experiment</u>		<u>Lithium (ng)</u>	<u>Boron (ng)</u>
1	Total (includes PBS)	176.85 ± .62	2001 ± 30
	PBS	128.27 ± .35	459 ± 46
	Difference	48.58 ± .71	1542 ± 55
	Expected from Plasma*	10.00 ± .48	630 ± 15
	Excess	38.58 ± .86	912 ± 57
	% Excess	485.79 ± 5.02	244.80 ± 4.29
2	Total (includes KCl)	48.48 ± .24	1670 ± 13
	KCl	3.17 ± .07	16 ± 2
	Difference	45.31 ± .25	1654 ± 13
	Expected from Plasma**	12.14 ± .23	586 ± 11
	Excess	33.17 ± .34	1068 ± 17
	% Excess	373.25 ± 1.97	282.13 ± 2.04

* Based on 1.649 g of dry plasma from 18.545 g wet plasma.

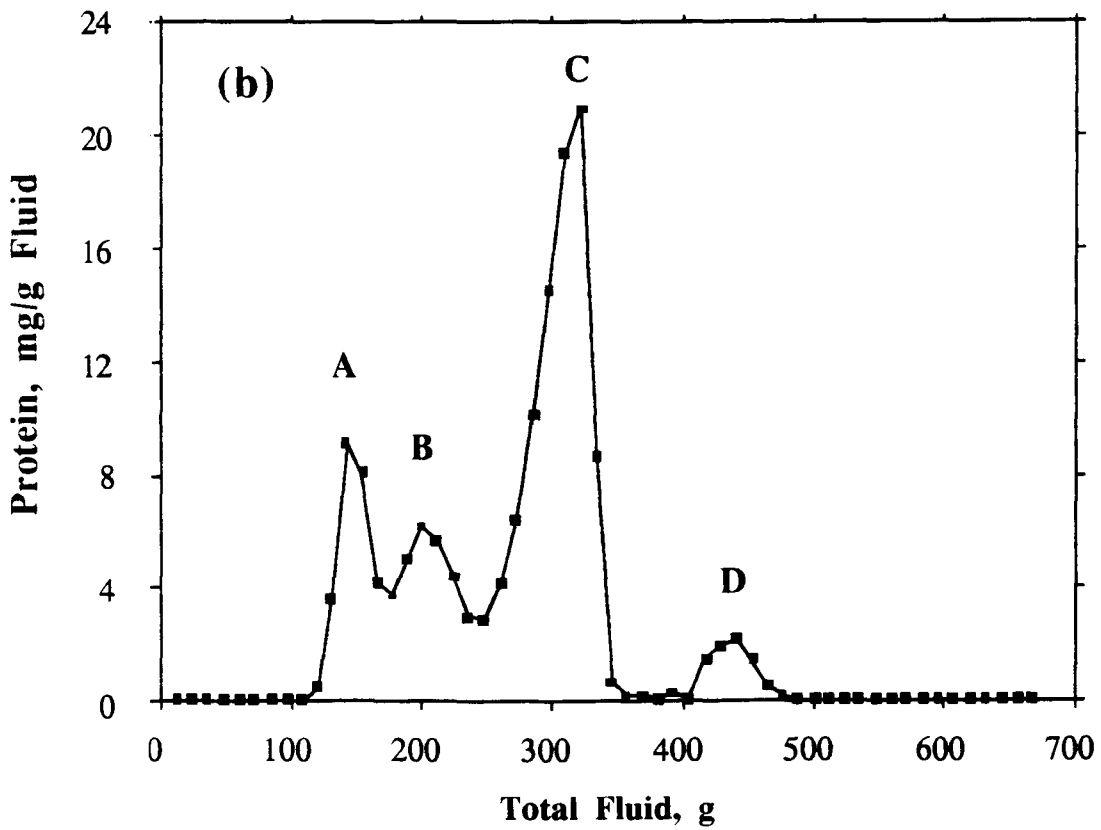
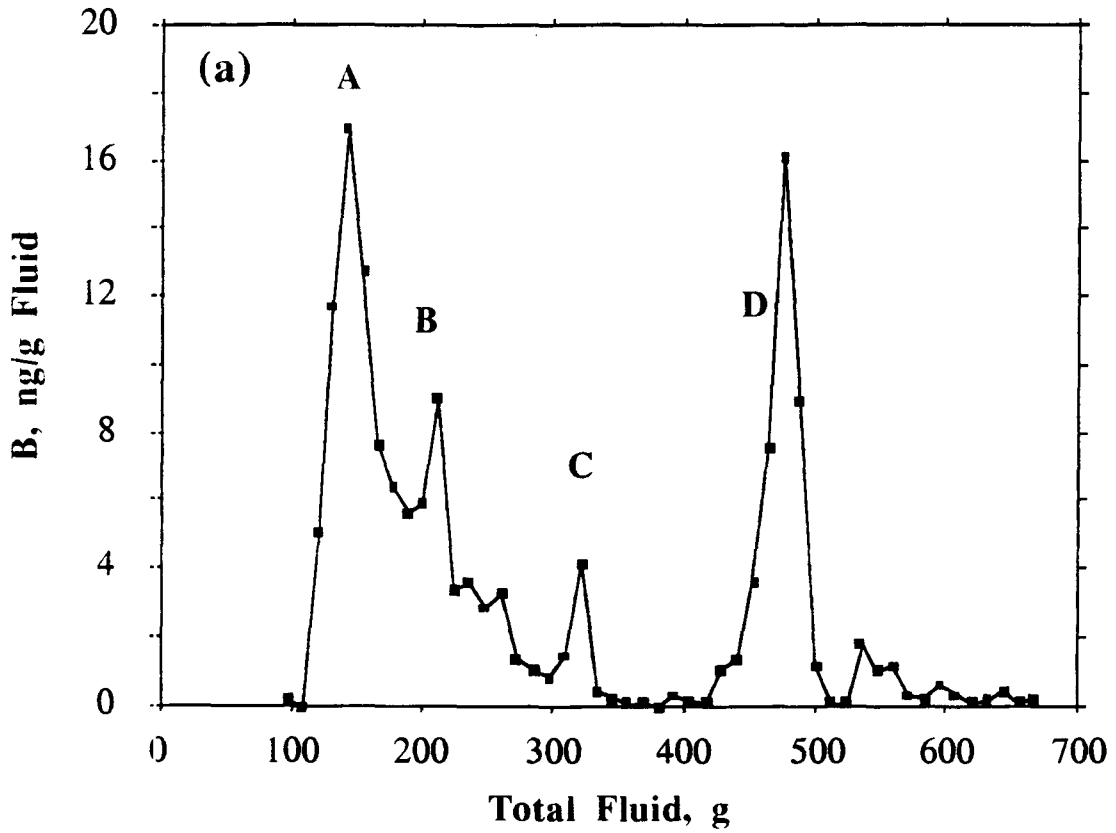
** Based on 1.912 g of dry plasma from 20.727 g wet plasma.

metals already in the gel, and not from metal deposited on the gel from the eluant. However, in the case of lithium, irradiation of Sephadex G-200 revealed that the gel contained very little lithium - about 0.36 ng/g of dry gel on average. Assuming about 15 g of gel in the column, the lithium naturally occurring in the gel amounts to only 5.4 ng. Referring to Table 3.3, this is not enough to account for all the excess lithium in the column fractions. Therefore, it must be concluded that either the proteins are taking lithium from both the eluant and the gel, or the lithium is deposited in the gel during column equilibration, from where it is later picked up by the proteins. The presence of the replacement peaks certainly suggests that lithium is being deposited on the gel. However, as noted above, the proteins do not necessarily take up all the lithium available. Thus, although the gel may bind lithium, in the case of experiment #1, it could not have bound all the lithium (estimated at 475 ng) made available to it during the column equilibration process.

Going on to the boron profile, it can be seen that the boron distribution follows a somewhat similar pattern to the lithium profile, in that the boron profile closely matches the protein peaks in position. However, it does not follow the protein profile in size. The boron is also more spread out over Peaks A, B and C, with no sharp divisions between the individual boron peaks, as observed in the lithium profile. Figure 3.4(a) is a plot of ng of boron/ g of fluid vs total fluid for the second experiment. Figure 3.5(a) is a similar plot of the boron profile from the first experiment. The boron background in the first experiment is estimated at about 120 ng/ dry g of PBS (1.14 ng/g of PBS solution), as opposed to the 7 ng/g (.042 ng/g of KCl solution) for the KCl. However, the boron profile in 3.5(a) is not so obscured by this higher background as the lithium profile in Figure 3.3(a).

As shown in Figure 3.4(a), the maximum of the boron peak associated with protein peak A coincides with the maximum of the lithium peak, but in peak B, the

Figure 3.4. (a) Boron profile for Gel Filtration Experiment #2, plotted as ng B/g fluid vs. total fluid (g). KCl background is included. Letters mark positions of the protein peaks. Boron peaks beyond large peak at **D** are replacement peaks.
(b) Protein profile for Gel Filtration Experiment #2.



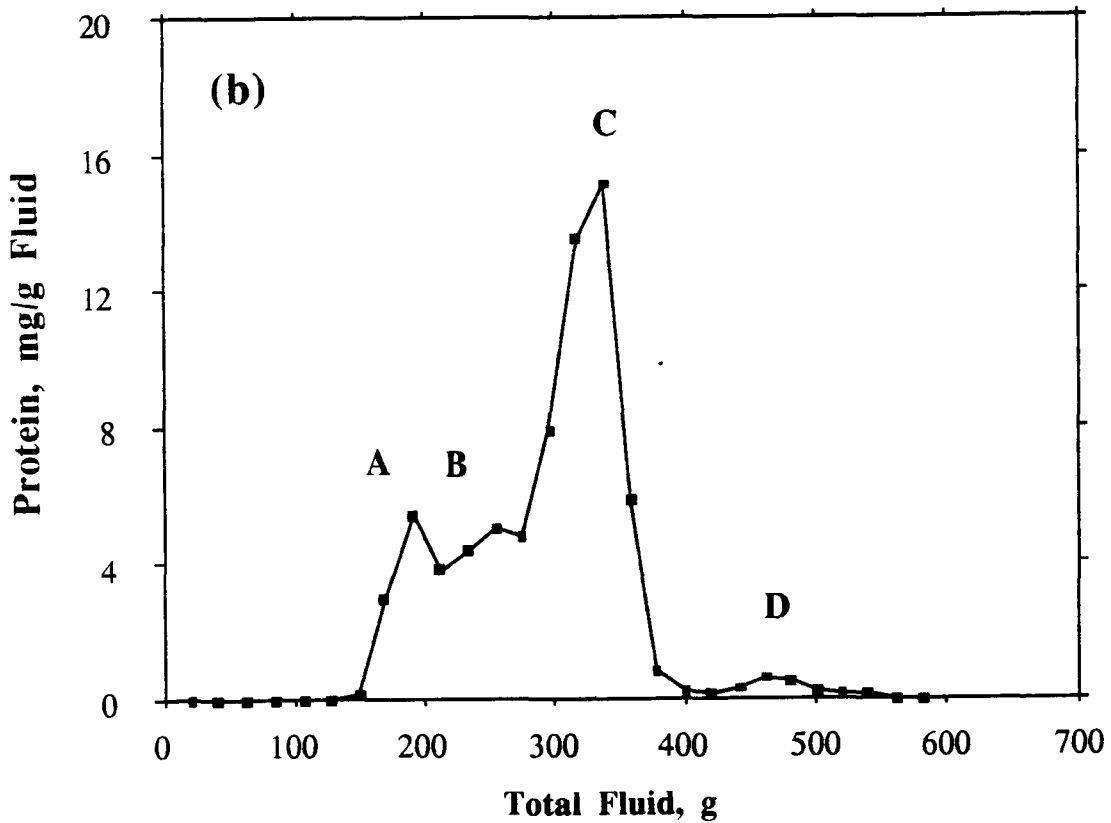
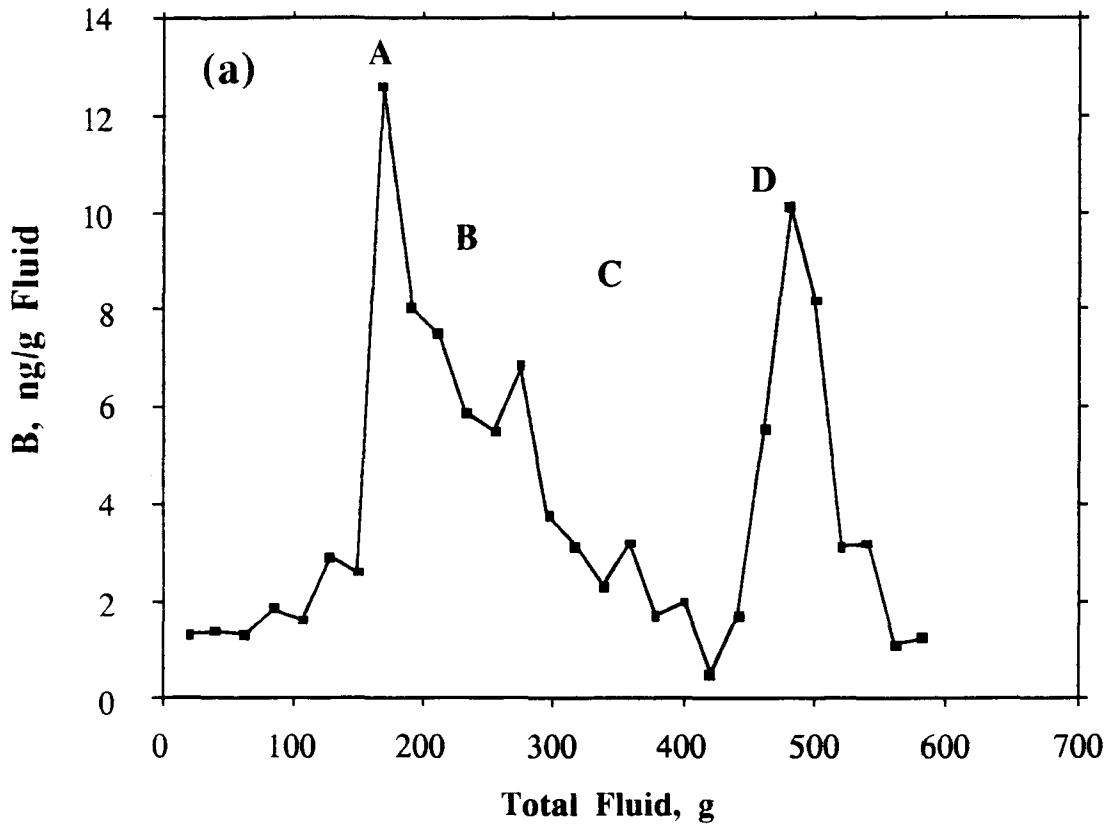
boron maximum is in a different fraction than the lithium maximum. There is also a boron peak in between peaks B and C, although it is not so well defined as the lithium peak. The fourth boron peak, in protein peak C, also coincides with its corresponding lithium peak. Peak D contains a very large amount of boron, and its distribution is somewhat different than the lithium in this region. Whereas the lithium was spread over all of Peak D, most of the boron is concentrated in the latter part of the peak. This may indicate that while most of the lithium is associated with low molecular weight substances, with a smaller amount as ions, much more of the boron may exist here as complex ions, rather than being bound to heavier molecules. Boron, being a non-metal, is not found in the ionic state as B^{+3} . Replacement peaks for boron, in the same positions as the lithium replacement peaks, are also in evidence.

The boron profile probably indicates the same kind of scavenging of boron from the gel as that of lithium, with the high molecular weight proteins picking up the most boron. However, in the case of boron, the scavenging seems to involve a much broader range of proteins, evidence that binding of boron is generally non-specific in nature. The only boron peak that appears to indicate more specific binding is the one associated with peak C, because of its narrow width, and its more distinct separation from the other boron peaks. The excess boron in both experiments is more than 200% of the expected amounts, as shown in Table 3.3, which is similar to the results reported by Gardiner et al.²⁸ for Zn^{+2} , Cu^{+2} and Fe^{+3} . Although the gel was found to contain large amounts of boron, about 7400 ng/dry g, most of it evidently washes out during the column equilibration process, since the percentage excess of boron is not as large as that for lithium, and in fact, is very nearly the same in both experiments, in spite of the much larger boron concentration in the PBS eluant compared to the KCl eluant. Further proof that

Figure 3.5. (a) Boron profile for Gel Filtration Experiment #1. PBS background is included. Letters show the positions of the protein peaks from Experiment #2 (see Figure 3.4 (b)).

(b) Protein profile for Gel Filtration Experiment #1. Letters show positions of protein peaks from Experiment #2 relative to the peaks in this figure.

52a



much of the boron washes out comes from a small batch (1 g) of dry gel which was soaked in distilled water for several days, with frequent changes of water, then freeze-dried and irradiated at McMaster. Subsequent mass spectrometry showed that the boron content was reduced by nearly 80%, on a dry weight basis, simply by soaking the gel for a relatively short time compared with the time taken for equilibration (three weeks).

3.7 Discussion

The results of the experiments show definitely that plasma proteins can bind lithium and boron. The specific proteins which bind these elements could not be precisely determined, but it is worthwhile to consider some possibilities. To this end, a closer examination of the lithium and boron profiles was made to try and determine how the binding of lithium and boron differed, and what the specific binding sites might be. This involved integration of the lithium, boron and protein peaks in order to determine the lithium/protein and boron/protein peak ratios. Results are given in Table 3.4 as ng Li (B)/mg protein.

From these ratios, the number of lithium (boron) atoms/protein molecule was calculated for a number of different protein molecular weights, ranging from 2.5×10^6 amu to < 5000 amu. These weights are not necessarily those of a specific protein, but were chosen to represent the general weight range in each peak. Integrations were done for the four lithium and boron peaks associated with the protein peaks, and for the ones in between peaks B and C. For these last lithium and boron peaks, integrations were done for the whole region, and for the two separate parts. As the analysis shows, proteins in all areas bind $\ll 1$ Li (B)/protein molecule, with the high molecular weight proteins in peak A binding the most lithium and boron. Only boron in the highest molecular weight range comes close

Table 3.4

Lithium/Protein and Boron/Protein Peak Ratios
Gel Filtration Experiment #2

<u>Protein Peak</u>	<u>Lithium Peak Ratios (ng Li/mg Protein)</u>	<u>Boron Peak Ratios (ng B/mg Protein)</u>
A	.034	2.228
B	.022	1.095
between B and C	.053	.685
between B and C (1st part)	.067	.946
between B and C (2nd part)	.045	.560
C	.013	.104
D*	.097	4.422

*"Protein" in this peak may include sugars and other low molecular weight complexes with lithium and boron, and ions.

<u>Protein Peak</u>	<u>Suggested Protein Wt (10^3 amu)</u>	<u>Li/1000 Protein Molecules</u>	<u>B/1000 Protein Molecules</u>
A	800 - 2500	3.9 - 12.2	165 - 515
B	150 - 250	0.5 - 0.8	15.2 - 25.3
between B and C	70 - 120	0.5 - 0.9	4.4 - 7.6
between B and C (1st part)	100	1.0	8.8
between B and C (2nd part)	80	0.5	4.1
C	50 - 70	0.09 - 0.13	0.5 - 0.7
D	< 5	< 0.07	< 2.0

1 Li atom = 6.94 amu

1 B atom = 10.81 amu

to one atom /molecule. The number of boron atoms/molecule was consistently higher than lithium in all areas, but this may simply be a result of more boron being available for binding. A similar set of integrations was not carried out for the first experiment, but it is interesting to speculate whether the lithium/protein ratios in particular would be higher because of the higher concentration of lithium available.

What the numbers in Table 3.4 suggest is that only a few of the protein molecules are binding lithium and boron, while the rest are binding none at all. This tends to support the hypothesis that only a small number of proteins are involved in lithium binding, so that the lithium/protein ratios given in Table 3.4 are too low, based as they are on the total estimated protein in the peak. For boron, the picture is less clear. The boron/protein ratios point to binding by only a few protein molecules, yet the boron profile, much more than the lithium profile, seems to indicate a non-specific type of binding, except perhaps in peak C.

In the case of lithium, it should be pointed out that, depending on which protein peak is considered, anywhere from ~ 82 - 10700 times (refer to Table 3.4) the amount of lithium already present would be required to give 1 Li/molecule for the type of non-specific binding discussed earlier. In other words, it would require μg amounts of lithium before this could occur. Even in experiment #1, where available lithium was much higher, there was not enough excess lithium to reach this level. In experiment #2, only an additional 36 ng of lithium were available from the KCl and the gel combined, compared to an estimated total of 720 ng in experiment #1.

However, it was calculated that only about 177 ng of lithium (including PBS) were recovered in experiment #1 (see Table 3.3), of which only 48.6 ng may actually be bound to the proteins. This suggests two possibilities: (1) that the proteins pick up lithium deposited on the gel, but the gel has only a limited capacity

for binding lithium, or (2) the proteins themselves are not very efficient at binding lithium, whatever the source, perhaps because of competition from other cations. If K^+ and Na^+ can displace Li^+ from the gel, they may also be able to displace it from proteins. These two ions are available in mg amounts in KCl and PBS solutions respectively.

Similar observations may apply to boron, since anywhere from 2 - 2080 times the available boron would be required for the non-specific binding of 1 atom/molecule. The proteins must also be picking up boron from the gel, since at least in the second experiment, only about 160 ng of boron were available from all the eluant passed through the column during equilibration and fraction collecting combined. Therefore, the rest must be from the gel. In experiment #1, about 2600 ng of boron is available from the PBS, yet the amount of boron recovered is not much greater than that recovered in experiment #2. Although the dry gel is very high in boron, it is evident that most of it washes out rapidly during equilibration. Otherwise, boron would be available to the proteins in μg quantities.

If only a few proteins are involved in the binding of lithium, as seems likely, the next step is to try and identify these proteins. Positive identification is not possible at this stage in the work, but a number of proteins suggest themselves. This is especially true in the area between peak B and C, since there are most likely only a small number of proteins here, and in peak C. Two possible candidates in the trough region between B and C are haptoglobin, a hemoglobin-binding protein of molecular weight 86 000, and the iron-binding protein transferrin, which has a molecular weight of 79 500 (see Table 3.2). In peak C, a likely protein is albumin, since it is known to bind a great variety of substances, including such metal ions as Ca^{+2} , Zn^{+2} , and Cu^{+2} and Mn^{+2} ⁷³. In the high molecular weight peak (peak A), a possible binding protein is α_2 -macroglobulin (MW = 725 000) and in peak B,

ceruloplasmin (MW = 132 000). In terms of the location of the lithium peaks, the proteins listed above are reasonable choices. The basis for this statement comes from the work of Pallon et al.³⁴, who also used Sephadex G-200 gel to investigate metal binding by proteins. In their illustrations, the location of zinc, which is known to bind to albumin and α_2 -macroglobulin, closely matched the location of lithium in our fractions. Similarly, they show copper, bound to ceruloplasmin, in the centre of the middle protein peak (peak B), which again corresponds well to the location of our second lithium peak. Transferrin was located on the right hand side of the trough between peaks B and C. The choice of haptoglobin was based on work by Killander⁵¹, who showed haptoglobin 1-1 to be right of centre in peak B. Having said this, there is still the problem that all the proteins listed so far are present in plasma in significant quantities (see Table 3.2), especially albumin, so that the ratio of 1 Li/molecule is still not possible. The only other alternatives are proteins which are present in very small quantities, perhaps only 1-3 mg/100 ml of plasma. A number of the more obscure plasma proteins exist in these quantities.

Specific binding proteins for boron are more difficult to determine, since the boron profile is more spread out over the protein fractions, with a distinct division only in the albumin peak (peak C). Therefore, albumin could be a likely binding protein. In the high molecular weight range, boron binding approaches 1 B/molecule, which may mean that at least in this region the binding of boron is really of a more non-specific nature than that of lithium.

As a final note, the lithium and boron peaks associated with peak D contain 10.2 ng of lithium and 466 ng of boron, which account for 84% of the lithium and 80% of the boron expected from the plasma. If this represents the situation *in vivo*, then at normal physiological levels of lithium and boron, very little of either element is bound by proteins. It is always possible, however, that a number of

proteins will bind lithium and boron if sufficient quantities are available, as for example, in the plasma of someone undergoing lithium therapy. Further investigation will be required to isolate the proteins, if any, which bind lithium and boron *in vivo*.

Chapter 4

Summary

In the course of this work, it has been demonstrated that the elements lithium and boron are capable of binding to plasma proteins. Although the specific proteins which bind these elements have not yet been positively identified, five possibilities for lithium, and one for boron have been suggested as a starting point for further investigation. It should be noted that the results obtained from the experiments may not necessarily reflect the situation *in vivo*, since considerably more lithium and boron were available than is normal in plasma.

Evidence from the lithium profile obtained from the second gel filtration experiment suggests that lithium may be bound to a small number of proteins, perhaps one in each of the three main protein peaks, and two in the trough between protein peaks B and C, at least *in vitro*. Two proteins which may be found in this trough area are transferrin, the major iron-binding protein in plasma, and one form of haptoglobin, a protein which binds hemoglobin. Other specific binding proteins might be α_2 -macroglobulin, a high molecular weight protein found in peak A, ceruloplasmin in peak B, and albumin in peak C.

The binding of boron to proteins appears to be more non-specific than that of lithium, with the high molecular weight proteins having the greatest ability to bind boron. One possibility of a specific binding protein is albumin, a protein which is known to bind a very large number of ions and molecules.

Other results include the concentration of lithium and boron in samples of whole blood, plasma and red blood cells, including two sets of samples from the same donor taken one year apart. Plasma from both of these sets was used in the gel filtration experiments. The data obtained from mass spectrometric analysis showed good agreement with some previously published data, but not with others. Analysis also showed that lithium and boron levels in plasma remain relatively constant in an individual over a long period of time. Lithium and boron ratios, defined as the ratio of lithium (boron) in red cell water to lithium (boron) in plasma water, also remained constant in the individual over the same period. The lithium ratios, which were <1.0 , confirmed previous work which showed that lithium is actively transported out of red blood cells by a $\text{Na}^+ - \text{Li}^+$ countertransport mechanism against its concentration gradient. The boron ratios for the donor whose plasma was used in the experiments was ~ 1 , suggesting that boron is evenly distributed between red cell and plasma water, although the boron ratio of a second donor was <1.0 . A wider range of samples will be needed in order to determine which of these ratios is correct.

A final result from the experiments is the observation that the published value for the cross section for the thermal reaction $^{39}\text{K}(n,\alpha)^{36}\text{Cl}$ must be significantly higher than the actual value. From irradiation of samples of KCl , a new estimate of $0.10 \pm .05$ mbarn was made for this cross section.

Bibliography

1. J.F.J. Cade, *Med. J. Aust.* **36**, 349 (1949).
2. J.F.J. Cade, in Lithium in Medical Practice, F.N. Johnson and S. Johnson, eds., (University Park Press, Baltimore, 1978).
3. M. Schou, *Pharmacol. Rev.* **9**, 17 (1957).
4. M. Schou, *Ann. Rev. Pharmacol.* **16**, 231 (1976).
5. F.N. Johnson, ed., Handbook of Lithium Therapy, (MTP Press Ltd., Lancaster, U.K., 1980). Includes a survey of books on lithium (pp.439-442).
6. F.N. Johnson, The History of Lithium Therapy, (MacMillan Press Ltd., London, 1984).
7. F.N. Johnson and S. Johnson, eds., Lithium in Medical Practice, (University Park Press, Baltimore, 1978).
8. M. Schou, *Psychopharmacol. Bull.* **5** (4), 33 (1969).
9. D.J. Kupfer, Lithium and Psychiatry Journal Articles, (Medical Examination Publishing Co., Inc., Flushing, N.Y., 1971).
10. B.K. Colasanti, in Modern Pharmacology, 2nd ed., C.R. Craig and R.E. Stitzel, eds., (Little, Brown and Company, Boston, 1986) pp. 543-545.
11. E.I. Hamilton, M.J. Minski. J.J. Cleary, *Sci. Tot. Environ.* **1**, 341 (1972).
12. W.B. Clarke, C.E. Webber, M. Koekebakker, R.D. Barr, *J. Lab. Clin. Med.* **109**, 155 (1987).

13. W.B. Clarke, M. Koekebakker, R.D. Barr, R.G. Downing, R.F. Fleming, *Appl. Radiat. Isot.* **38**, 735 (1987).
14. E. Bourret, I. Moynier, L. Bardet, *Analyt. Chim. Acta* **172**, 157 (1985).
15. S. Luan, X. Shan, Z. Ni, *J. Analyt. At. Spectrom.* **3**, 989 (1988).
16. R. Zaldivar, *Arch. Environ. Toxicol.* **46**, 319 (1980).
17. W.B. Clarke, R.S. Gibson, *J. Food Comp. Anal.* **1**, 209 (1988).
18. W. Mertz, *Science* **213**, 1332 (1981).
19. M. Anke, B. Groppe, H. Kronemann, in Trace Element Analytical Chemistry in Medicine and Biology, vol. 3, P. Bratter and P. Schramel, eds., (Walter de Gruyter, Berlin, 1984) pp. 421-451.
20. E. Frieden, ed., Biochemistry of the Essential Ultratrace Elements, (Plenum Press, New York, 1984).
21. E.L. Pratt, E.E. Pickett, B.L. O'Dell, *Bioinorg. Chem.* **9**, 299 (1978).
22. J. Burt, PhD Thesis, University of Missouri - Columbia (1982).
23. E.E. Pickett, *Spurenelementsymposium*, Karl Marx University, Leipzig and Friedrich Schiller University, Jena, East Germany (1983).
24. R.D. Barr, M. Koekebakker, E.A. Brown, M.C. Falbo, *J. Lab. Clin. Med.* **109**, 159 (1987).
25. R.D. Barr, P.R. Galbraith, *Can. Med. Assoc. J.* **128**, 123 (1983).
26. various articles in R.R. Crichton, ed., Proteins of Iron Storage and Transport in Biochemistry and Medicine, (North-Holland Publishing Co., Amsterdam, 1975).
27. E.J. Underwood, Trace Elements in Human and Animal Nutrition, 4th ed., (Academic Press, New York, 1977).
28. P.E. Gardiner, J.M. Ottaway, G.S. Fell, R.R. Burns, *Analyt. Chim. Acta* **124**, 281 (1984).

29. M. Cochran, S. Neoh, E. Stephens, *Clin. Chim. Acta* **132**, 199 (1983).
30. G.A. Trapp, *Life Sci.* **33**, 311 (1983).
31. H. Rahman, A.W. Skillen, S.M. Channon, M.K. Ward, D.N.S. Kerr, *Clin. Chem.* **31**, 1969 (1985).
32. M. Cochran, D. Patterson, J.H. Coates, P.T.H. Coates, in Trace Element Analytical Chemistry in Medicine and Biology, vol. 3, P. Bratter and P. Schramel, eds., (Walter de Gruyter, Berlin, 1984) pp. 311-318.
33. R.J. Shamberger, in Biochemistry of the Essential Ultratrace Elements, E. Frieden, ed., (Plenum Press, New York, 1984) p. 223.
34. J. Pallon, P. Pakarinen, K. Malmqvist, K.R. Akselsson, *Biol. Trace Elem. Res.* **12**, 401 (1987).
35. F.H. Nelson in, Biochemistry of the Essential Ultratrace Elements, E. Frieden, ed., (Plenum Press, New York, 1984) pp 294-295.
36. J.C. Cannon, N.D. Chasteen, in Proteins of Iron Storage and Transport in Biochemistry and Medicine, R.R. Crichton, ed., (North-Holland Publishing Co., Amsterdam, 1975) pp. 67-72.
37. C.W. Carr, *Arch. Biochem. Biophys.* **62**, 476 (1956).
38. C.W. Carr, W.P. Engelstad, *Arch. Biochem. Biophys.* **77**, 158 (1958).
39. E.J. Cohn, F.R.N. Gurd, D.M. Surgenor, B.A. Barnes, R.K. Brown, G. Derouaux, J.M. Gillespie, F.W. Kahnt, W.F. Lever, C.H. Liu, D. Mittelman R.F. Mouton, K. Schmid, E. Uroma, *J. Am. Chem. Soc.* **72**, 465 (1950).
40. S. Kaufman, *Meth. Enzymol.* **22**, 233 (1971).
41. P.J. Talso, R.W. Clarke, *Am. J. Physiol.* **166**, 202 (1951).
42. J. Foulkes, G.H. Mudge, A. Gilman, *Am. J. Physiol.* **168**, 642 (1952).
43. R.J. Baldessarini, in The Pharmacological Basis of Therapeutics, 6th ed.,

- A. Goodman Gilman, L.S. Goodman, A. Goodman, eds., (MacMillan Publishing Co., Inc., New York, 1980) pp. 430-434.
44. M. Schou, *Clin. Pharmacokin.* **15**, 283 (1988).
 45. E. Hove, C.A. Elvehjem, E.B. Hart, *Am. J. Physiol.* **127**, 689 (1939).
 46. H.R. Imbus, J. Cholak, L.H. Miller, T. Sterling, *Arch. Environ. Health* **6**, 286 (1963).
 47. C.J. Lovatt, W.M. Dugger, in Biochemistry of the Essential Ultratrace Elements, E. Frieden, ed., (Plenum Press, New York, 1984) pp. 394-396.
 48. P. Andrews, *Biochem. J.* **96**, 595 (1965).
 49. Gel Filtration: Theory and Practice, Pharmacia Laboratory Separation Division, (Uppsala, Sweden) no date.
 50. J. Pallon, P. Pakarinen, R. Akselsson, *Nucl. Inst. Meth. Phys. Res.* **B3**, 373 (1984).
 51. J. Killander, *Biochim. Biophys. Acta* **93**, 1 (1964).
 52. G.W. Evans, P.E. Johnson, J.G. Bushmiller, R.W. Ames, *Analyt. Chem.* **51**, 839 (1979).
 53. P. E. Gardiner, E. Rosick, U. Rosick, P. Bratter, G. Kynast, *Clin. Chim. Acta* **120**, 103 (1982).
 54. P. E. Gardiner, M. Stoepler, H.W. Nurnberg, in Trace Element Analytical Chemistry in Medicine and Biology, vol. 3, P. Bratter and P. Schramel, eds., (Walter de Gruyter, Berlin, 1984). pp. 299-310.
 55. B.M. Oliver, H. Farrar IV, M.M. Bretscher, *Appl. Radiat. Isot.* **38**, 959 (1987).
 56. IUPAC Subcommittee on Assessment of Isotopic Composition of the Elements, *Pure & Appl. Chem.* **56**, 695 (1984).
 57. D.A. Becker, *J. Radioanal. Nucl. Chem.* **110**, 393 (1987).

58. B.L. Cohen, in Handbook of Radiation Measurement and Protection, A.E. Brodsky, ed., (CRC Press Inc., West Palm Beach, FL, 1978) pp. 91-212.
59. V. McLane, C.L. Dunford, P.F. Rose, Neutron Cross Sections, vol. 2, (Academic Press, New York, 1988) pp. 35-49.
60. S.F. Mughabghab, M. Divadeenam, N.E. Holden, Neutron Cross Sections, vol. 1, (Academic Press, New York, 1981).
61. J. Benisz, A. Jasielska, T. Panek, *Acta Phys. Pol.* **28**, 763 (1965).
62. C. Hanna, D.B. Primeau, P.R. Tunnicliffe, *Can. J. Phys.* **39**, 1784 (1961).
63. E. Munnich, *Z. Phys.* **153**, 106 (1958).
64. W.S. Snyder, M.J. Cook, L.R. Karhausen, G.P. Howells, I.H. Tipton, Report of the Task Group on Reference Man, ICRP report no. 23, (Pergamon Press, New York, 1975).
65. W.B. Clarke, W.J. Jenkins, *Z. Top, Appl. Radiat. Isot.* **27**, 515 (1976).
66. W.J. Jenkins, PhD. Thesis, McMaster University, 1974.
67. G. Erdtmann, W. Soyka, The Gamma Rays of the Radionuclides, (Verlag Chemie, New York, 1979).
68. W.B. Clarke, R.F. Fleming, *Phys. Rev. C* **39**, 1633 (1989).
69. B.E. Ehrlich, J.M. Diamond, V. Fry, K. Meier, *J. Membrane Biol.* **75**, 233 (1983).
70. T. Scott, M. Eagleson, eds., Concise Encyclopedia Biochemistry, 2nd ed., (Walter de Gruyter, Berlin, 1988) p. 342
71. F.W. Putnam, ed., The Plasma Proteins, Structure, Function and Genetic Control, 2nd ed., vol. IV, (Academic Press, Orlando FL, 1984) pp 5-8, 17.
72. D.J.R. Evans, K. Fritze, *Analyt. Chimica Acta* **44**, 1 (1969).
73. G.D. Fasman, ed., Handbook of Biochemistry and Molecular Biology: Proteins, 3rd ed., vol II, (CRC Press, Cleveland, 1976) pp 554-582.